REC-OCE-69-5

EXPERIMENTAL STUDY AND ANALYSIS OF DRAFT-TUBE SURGING

Dr. J. J. Cassidy
Division of Research
Office of Chief Engineer
Bureau of Reclamation

October 1969

U. S. Department of the Interior
Bureau of Reclamation

REC-OCE-69-5
Report No. HYD-591

EXPERIMENTAL STUDY AND ANALYSIS OF DRAFT-TUBE SURGING

by
Dr. J. J. Cassidy

October 1969

HYDRAULICS BRANCH
DIVISION OF RESEARCH

UNITED STATES DEPARTMENT OF THE INTERIOR * BUREAU OF RECLAMATION
Office of Chief Engineer . Denver, Colorado

ACKNOWLEDGEMENTS

This study was conducted while the writer (Professor of Civil Engineering, University of Missouri, Columbia, Missouri) was a Ford Foundation Engineer Resident with the Hydraulics Branch, Division of Research. Design of experimental equipment was performed primarily by Dr. H. T. Falvey. Mr. U. J. Palde collected a portion of the data while Mr. W. M. Batts performed the photography. Turbine performance data and advice relative to hydraulic machinery were furnished by Mr. C. G. Bates and Mr. G. H. Johnson, Hydraulic Machinery Branch, Division of Design. The manuscript was reviewed critically by Dr. H. T. Falvey. Head, Hydraulics Research Section. The entire project was under the direction of Mr. H. M. Martin, Hydraulics Branch Chief.

CONTENTS

Page

Abstract ii
Nomenclature iv
Purpose 1
Conclusions 1
Applications 1
Introduction 1
Equipment 2
Analysis 3
Experimental Procedure 4
  The Onset of Surging 4
  Frequency and Amplitude of Surging 4
  Tubes Studied 4
  Flow Visualization 4
Discussion of Results 4
  Influence of Viscosity 4
  Nature of the Onset of Surging 4
  Frequency and Pressure Characteristics 5
Application to Hydraulic Turbines 6
  Analysis 6
  Effect of Tailwater 7
Model-Prototype Similitude 8

Figures

Effect of Rotation on Flow Pattern 1
Experimental Apparatus 2
Schematic Diagram of Apparatus 3
Smoke Generator 4
Photographs of Flow Patterns 5
Photographs of Flow Patterns 6
Draft Tubes and Flow Patterns 7
Critical Values of $\Omega D/\rho Q^2$ 8
Velocity and Pressure Traces Photographed on the Oscilloscope 9
Frequency Parameter as a Function of Reynolds Number for Straight Tubes 10
Pressure Parameter as a Function of Reynolds Number for Straight Tubes 11
Frequency Parameter as a Function of Reynolds Number for the Fontenelle Draft Tube . . . 12
Frequency Parameter for all Tubes as a Function of Momentum Parameter 13
Pressure Parameter for all Tubes as a Function of Momentum Parameter 14
Velocity Diagrams for a Turbine Runner 15
Operating Characteristics for Fontenelle Model Turbine 16
Efficiency Hill-Hoover Replacement-Runner Model Data 17
Hoover Model Data—Frequency, Momentum, σ 18
Hoover Replacement-Runner Model Data, Pressure Parameter Versus Momentum Parameter for Various Values of σ 19
Schematic Diagram of Velocity Vectors on Wicket Gates and the Runner 20

ABSTRACT

Draft-tube surge experiments were conducted with models of draft tubes, using air as the fluid. The occurrence, frequency, and amplitude of surges were correlated with flow and draft-tube geometry variables. Studies show that surges arise when angular momentum reaches a critical value relative to linear momentum. Surge frequency and peak-to-peak pressures are independent of viscous effects for Reynolds numbers above 80,000, and are correlated with a dimensionless momentum parameter for a particular draft-tube shape. A criterion is given for predicting the surging threshold. Results of the study are applied to analysis of draft-tube surging in the Fontenelle and Hoover replacement turbines.

DESCRIPTORS--/ *draft tubes/ *turbines/ *hydroelectric plants/ hydraulic machinery/ fluid mechanics/ dimensional analysis/ *surges/ air/ unsteady flow/ pressure/ laboratory tests/ model tests/ fluid flow/ non-uniform flow
IDENTIFIERS--/ fluid dynamics/ hydraulic resonance

Where approximate or nominal English units are used to express a value or range of values, the converted metric units in parentheses are also approximate or nominal. Where precise English units are used, the converted metric units are expressed as equally significant values. A table of conversion factors—BRITISH TO METRIC UNITS OF MEASUREMENT—is provided at the end of this report.

NOMENCLATURE

Unless otherwise noted, all dimensions are in the foot-pound-second (meter-kilogram-second) system.

A = area

B = height of wicket gates

D = diameter of draft-tube throat

D_R = runner diameter at midpoint of wicket gates

H = net head across turbine

H_B = atmospheric pressure head minus vapor pressure head

H_S = static draft head on turbine (negative for turbines set above tailwater)

L = length of draft tube

P = power

ΔP = peak-to-peak value of pressure surge

Q = discharge

R = Reynolds number = WD/ν

V = velocity

$W = Q/A$ = average axial velocity

f = frequency

f_n = natural frequency

g = acceleration due to gravity

n = rotation speed (rev/sec)

r = coordinate in radial direction

u = velocity component in radial direction

v = velocity component in peripheral direction

w = velocity component in axial direction

z = coordinate in axial direction

Ω = rate of flow of angular momentum

γ = specific weight

$\phi = \dfrac{\pi Dn}{60\sqrt{2gH}}$ = peripheral speed coefficient; also, a function

α = angle between a radial line and velocity vector

θ = coordinate angle in cylindrical coordinate system

ν = kinematic viscosity of fluid

π = 3.1416

ρ = fluid density

$\sigma = (H_B - H_S)/H$ = turbine cavitation number

ω = angular velocity (rad/sec)

PURPOSE

The analysis and experimental investigation were conducted in order to gain an understanding of draft-tube surging and to correlate occurrence, frequency, and amplitude of draft-tube surges with flow and geometric variables involved in turbine and draft-tube flow.

CONCLUSIONS

1. Draft-tube surges are a stable unsteady form of flow arising when the rate of flow of angular momentum reaches a critical value relative to the rate of flow of linear momentum. The dimensionless momentum parameter $\Omega D/\rho Q^2$ has a critical value above which surging exists.

2. Frequency and peak-to-peak values of draft-tube pressure surges are independent of viscous effects for Reynolds numbers above approximately 80,000. Prototype Reynolds numbers greatly exceed 80,000.

3. Dimensionless parameters for peak-to-peak pressures and frequency of draft-tube surging can be correlated with a dimensionless momentum parameter for a particular draft-tube geometry.

APPLICATIONS

The results of this study can be applied to the analysis of flow through turbine draft tubes, or conceivably, to flow through pump intakes. The surge frequency and amplitude predicted by similitude yield reasonable prototype values. If the analysis for turbines is fully developed, designers could conceivably predict in advance operational conditions at which surging would occur for a particular unit. However, it would be highly desirable to correlate the results of this study with the frequency, amplitude, and threshold of surging observed in a carefully planned prototype observation, one in which discharge, head, gate, plant sigma, and turbine geometry as well as surge characteristics are observed or known.

INTRODUCTION

Draft-tube surges have been observed in hydroelectric plants using Francis-type turbines apparently since the time these units first went into operation.[1] Effects of surges have been observed as power swings or general noise and vibration. In most cases powerplant operators rapidly learn where the "rough" areas of operation are and avoid operation in those regions. In some cases vertical vanes are spaced around the periphery of the draft-tube entrances in an attempt to modify or eliminate the swirl in the flow and thus reduce the severity of, or eliminate, surging. Air is also frequently admitted below the runner to "smooth out" operation.

The phenomenon of surging is known to be due to rotation of flow passing through the draft tube. Pictures of the helical vortex thus generated have been taken by Wigle[2] and Hosoi[3] to mention only two. However, very little in the way of quantitative information, useful to the engineer, is currently available beyond the equation proposed by Rheingans[1] for the expected frequency of the surge:

$$f = \frac{n}{3.6}$$

f is the surge frequency in cycles per second and n is the turbine rotational speed in revolutions per second.

Purely axial flow through a straight tube is stable once the transition to a fully turbulent flow takes place. If some rotation is superimposed on this flow, however, the flow pattern makes a drastic change from that of the purely axial flow.[4] The axial velocity decreases on the centerline and increases near the wall. The peripheral component of velocity also increases near the wall. Figure (1) shows a typical velocity distribution in axial and axial-with-rotation flows. If the discharge is kept constant and the rotational velocity of the flow is increased, a radical change in flow pattern occurs. A reversal in flow takes place at the tube axis and a stagnation point is developed on the centerline. On the centerline, flow is toward the stagnation point from both the upstream and downstream directions. The development of reversed flow along the axis of the tube has been referred to as vortex breakdown.[6]

Basic investigation of this vortex breakdown first occurred not as a result of interest on the part of turbine users or manufacturers, but rather as the result

[1] Rheingans, W. J., "Power Swings in Hydroelectric Power Plants," Trans. ASME, Vol. 62, 1940.
[2] Wigle, D. A., et al, "Hydraulic Model Studies for Turbines at Grand Coulee Powerplant," U.S. Bureau of Reclamation, Hydraulic Laboratory Report, HYD-198, Denver, Colorado, 1946.
[3] Hosoi, Y., "Experimental Investigations of Pressure Surge in Draft Tubes of Francis Water Turbines," Hitachi Review, V. 14, No. 12, 1965.
[4] Kreith, F. and O. K. Sonju, "The Decay of a Turbulent Swirl in a Pipe," JOURNAL OF FLUID MECHANICS, Vol. 22, Part 2, 1965.
[6] Benjamin, T. B., "Theory of the Vortex Breakdown Phenomenon," JOURNAL OF FLUID MECHANICS, Vol. 14, 1962.

of observations made by people interested in acoustics[5] and the "breakdown" observed on the vortices forming above delta wings on high-speed modern airplanes.[6]

The analytical study by Benjamin[6] indicated that the "breakdown" was actually a transition from one stable regime of flow to another. He showed that prior to the breakdown an axisymmetric standing wave could not exist in the flow while the breakdown produced a flow which could support such a wave. Benjamin used the well-understood hydraulic jump as an analogy to what occurred in the vortex breakdown.

Quantitative information on the occurrence of vortex breakdown was apparently first obtained by Squire[7] in an analytical study. According to Squire's theory, breakdown occurred when the maximum swirl angle (the angle whose tangent is v/w - See Figure 1) was 52^{o} or greater.

Harvey[8] in an experimental study using air flowing through a straight tube measured a maximum swirl angle of 51^{o} using smoke injected in the flow just upstream from the breakdown.

If, after breakdown has occurred, the rotational velocity of the fluid is further increased, the flow downstream from the point of transition forms a precessing helical vortex. It is the precession of this vortex which produces the pressure surge. This aspect of the phenomenon, which is the most important to the engineer, has received very little basic investigation.

Chanaud[9] studied both the steady and unsteady part of the transition. He found that the Strouhal number fD/W (D is tube diameter and W is the average axial velocity) of the precessing vortex depended upon the tube length to diameter ratio L/D and the axial Reynolds number of the flow. Unfortunately, Chanaud's data regarding rotation are in error because he assumed that the flow moving through a revolving tube was set into rigid body motion equivalent to that of the pipe. However, qualitatively his results are of considerable interest. He found that the transition to helical-spiral (surging) flow took place more readily at larger Reynolds numbers. For Reynolds numbers below 250 unsteady flow could not be produced in the tube regardless of the degree of rotation imparted to the fluid.

Quantitative information regarding both the onset of surging and the characteristics of frequency and amplitude of the resultant surge would be of considerable value to the engineer concerned with design and selection of hydraulic machinery. This study was designed to produce both qualitative information on the nature of surges in contemporary turbine draft tubes, and to obtain quantitative information on occurrence and characteristics of surge frequency and amplitude.

EQUIPMENT

For the sake of convenience, it was decided to conduct the experiments with air as the fluid medium. The apparatus is shown in photographs in Figure 2 and schematically in Figure 3. Because a study involving a model of the Fontenelle draft tube and spiral case had been previously conducted, many of the details of the experimental apparatus were actually scale models of corresponding Fontennelle components[10].

Because the phenomena is quite complex at best, it was highly desirable, at least for this initial study, to simplify the geometry as much as possible. Hence, no turbine runner was to be installed in the draft tube. Rotation was introduced as the flow passed through inclined vanes in the radial approach to the draft tube. Radial inclination of these vanes was readily adjusted by a control extending outside the stilling chamber. With this control the angle between the gates and a radial line could be set at any value between 0^{o} and 52.5^{o}. At 0^{o} the gates are fully open and no rotation is imparted to the flow.

Discharge was controlled by the motor-driven cone valve at the entrance to the stilling chamber and computed from the differential pressure across the orifice in the supply line. The supply line leading from the fan to the stilling chamber had a 9.952-inch inside diameter and the orifice diameter was 4.801 inches. Pressure differential across the orifice was measured using a calibrated 2.5 psig Statham pressure cell.

Piezometers (1/16 inch in diameter) were installed in the draft tubes for the measurement of peak-to-peak pressures of the surges. A 2.5 psig Statham pressure cell was used as a transducer for the pressure surges. After amplification, the signal from the pressure cell was displayed on an oscilloscope equipped with a variable

[5] Chenaud, R. C., "Experiments Concerning the Vortex Whistle," JOURNAL OF THE ACOUSTICAL SOCIETY OF AMERICA, Vol. 35, No. 7, 1963.
[7] Squire, H. B., "Analysis of the Vortex Breakdown Phenomenon, Part I," Aero, Dept., Imperial College, Rep. No. 102, 1960.
[8] Harvey, J. K., "Some Observations of the Vortex Breakdown Phenomenon," JOURNAL OF FLUID MECHANICS, Vol. 14, 1962.
[9] Chenaud, R. C., "Observations of Oscillatory Motion in Certain Swirling Flows," JOURNAL OF FLUID MECHANICS, Vol. 21, 1965.
[10] Falvey, H. T., "Hydraulic Model Studies of the Fontenelle Powerplant Draft Tube and Tailrace," Report No. Hyd-571, U.S. Bureau of Reclamation, Denver, Colorado, August 1967.

persistence screen. With the variable persistence feature it was possible to retain as many traces as desired and then store the result as a permanent image. When stored, the resultant image was static and could be scrutinized for frequency and peak-to-peak value.

Taps were also mounted on the draft tubes so that velocity measurements could be made using a hot-film anemometer. The signal from the anemometer could also be displayed on the oscilloscope. Calibration of the hot-film was accomplished by placing the probe in an air jet, the velocity of which had been measured using a stagnation tube and a differential manometer.

ANALYSIS

In order to be able to utilize the results of this study in an actual hydraulic-turbine application, it was necessary to generalize the results in a basic fashion. Complete analytical solution to the problem of draft-tube surging would naturally provide the necessary generalization. However, such a solution seems as yet to be unattainable. An experimental study was therefore indicated.

When faced with the need to generalize experimental results, dimensional analysis can be very useful if the phenomenon is at least partially understood.

In this case, the assumption was made that the frequency of the surge is a function of only the fluid density ρ, the fluid viscosity ν, the draft tube diameter D and Length L, the discharge Q, and the rate of flow of angular momentum Ω. Thus,

$$f = \phi\ (\rho, \nu, D, L, Q, \Omega) \tag{2}$$

Application of standard techniques of dimensional analysis to Equation (2) produces

$$\frac{fD^3}{Q} = \phi_1\left(\frac{\Omega D}{\rho Q^2}, \frac{L}{D}, \frac{Q}{D\nu}\right) \tag{3}$$

as one possible set of dimensionless parameters. The frequency parameter is actually a form of Strouhal number written in terms of discharge rather than mean velocity. The first parameter on the right of Equation (3) is a dimensionless ratio of angular-momentum flux to linear-momentum flux. If the discharge is held constant and angular-momentum flux is increased for a particular tube the magnitude of the momentum parameter is increased. The last parameter on the right of Equation (3) is simply the Reynolds number and will be represented as R = WD/ν throughout the remainder of this report.

The peak-to-peak value ΔP of the pressure produced at a particular point by the surge can be assumed to be a function of the same variables as the frequency. Thus,

$$\Delta P = \phi_2\ (\rho, \nu, D, L, Q, \Omega) \tag{4}$$

or in one possible combination of dimensionless terms

$$\frac{\Delta P D^3}{\Omega} = \phi_3\ (\frac{\Omega D}{\rho Q^2}, \frac{L}{D}, R) \tag{5}$$

Two things should be noted at this point. First, the role of draft-tube shape cannot be incorporated in this type of analysis and data plotted according to Equations (3) and (5) will produce different results for each tube shape tested. Second, the parameter $\Omega D/\rho Q^2$ is obviously a gross parameter quite in contrast to the local swirl angle $\tan^{-1}\frac{V}{W}$ as used by previous analysts and experimenters. Because of its gross feature, this momentum parameter is easily utilized, but in utilizing it, the assumption must be made that regardless of the manner in which angular momentum is introduced into the flow the resulting flow pattern will be the same as long as $\Omega D/\rho Q^2$ is constant.

With the exception of Ω all variables in Equations (3) and (5) could be measured directly with the experimental equipment. The flux of angular momentum was computed from the geometry of the inlet to the draft tube as follows:

From the gate diagram (see Figure 20)

$$Q = \int V_o \cos\alpha\, dA = \int_0^{2\pi} V_o Br \cos\alpha\, d\theta$$

where B is the height of the wicket gates.

Also,

$$\Omega = \rho \int V_o \cos\alpha\, (rV_o \sin\alpha) dA = \int_0^{2\pi} \rho V_o^2 Br^2 \cos\alpha \sin\alpha\, d\theta$$

Assuming that V_o, B, and r are constant with respect to θ

$$Q = V_o \cos\alpha\, 2\pi rB$$

$$\Omega = \rho V_o^2 \cos\alpha \sin\alpha\, 2\pi r^2 B$$

Thus,

$$\frac{\Omega D}{\rho Q^2} = \frac{D \tan\alpha}{2\pi B} \tag{6}$$

Hence, the momentum parameter is a function of only the gate opening, draft-tube inlet diameter, and height of gates.

EXPERIMENTAL PROCEDURE

A. THE ONSET OF SURGING

A qualitative and quantitative description of the transition from steady uniformly-swirling flow to unsteady surging flow was obtained by two separate experimental methods. At average velocities below 5 fps (1.64 m/s) smoke was injected on the centerline of the tube at the upstream cover. The gate angle--and thus $\Omega D/\rho Q^2$ --at which the transition took place was recorded. Because the longitudinal location of the transition point moved upstream as $\Omega D/\rho Q^2$ was increased, two critical values of the momentum parameter were recorded: (1) When the transition occurred just within the tube exit; and (2) when surging occurred throughout the tube.

A hot-film anemometer was used to detect transition to surging at high average flow velocities. A cylindrical hot-film probe was positioned at the centerline near the tube exit. Flow was established with no rotation. Then $\Omega D/\rho Q^2$ was gradually increased (by closing the wicket gates). The value of $\Omega D/\rho Q^2$ at which a reversal in velocity was noted at the centerline was recorded as the critical value. At these large velocities, transition appeared to progress rapidly upstream. Two critical values were not observed since flow seemed to become unsteady throughout the entire tube almost simultaneously.

B. FREQUENCY AND AMPLITUDE OF SURGING

Two separate measurements were made of surge frequency. Using the previously described pressure cell to detect pressure surging and cylindrical hot-film probe to detect velocity near the piezometer, traces of velocity and pressure were displayed simultaneously on the dual-beam oscilloscope. Figure (9) is a picture of two traces thus made. Approximately 50 traces of both velocity and pressure were retained for the photograph in Figure (9) through use of the persistence feature of the oscilloscope screen.

Peak-to-peak pressures were obtained by measuring the peak-to-peak voltage of the oscilloscope display and relating this to the calibrated output of the pressure cell and its associated amplifier.

Experimental procedure was the same for each tube. A particular gate angle was set with maximum obtainable discharge (approximately 10 ft^3/sec-- 0.283 m^3/sec). The discharge was then successively decreased in small increments by closing the cone valve. Frequency and peak-to-peak pressures were measured and recorded for each discharge.

C. TUBES STUDIED

Straight tubes studied included two different diameters--6.13 inches (15.56 cm), 3.44 inches (8.76 cm)--with lengths giving rise to L/D ratios ranging from 1.63 to 7.20. In addition, a model of the Fontenelle draft tube with a throat diameter of 6.13 inches (15.26 cm) and a straight cone having the same expansion ratio, throat diameter, and centerline length as the draft tube were also studied. All tubes were formed from transparent plexiglass in order to facilitate flow visualization. The draft tube can be seen in Figure (2) and the remaining tubes studied are shown in Figure (7).

D. FLOW VISUALIZATION

Smoke was chosen as the most desirable agent for obtaining flow visualization for this particular study. After some experimentation, pipe tobacco proved to produce the least objectionable of the varieties of smoke which were dense enough to provide good visualization. The smoke generator developed for this study is shown schematically in Figure (4).

DISCUSSION OF RESULTS

A. INFLUENCE OF VISCOSITY

Figures 10, 11, and 12 show dimensionless frequency and pressure plotted against Reynolds number for straight pipes and the Fontenelle draft tube. The frequency and pressure parameters are both seen to be essentially constant for Reynolds numbers beyond 80,000. Since a prototype hydraulic turbine would have a Reynolds number well above this (for Fontenelle design conditions R = 18,600,000) viscosity does not seem to be an important variable in surging of hydraulic turbines.

B. NATURE OF THE ONSET OF SURGING

As pointed out in the introduction, most investigators have utilized the magnitude of the swirl angle as the predictor of the onset of vortex breakdown. In each case observed here the breakdown began at the center of the pipe. Invariably the maximum swirl angle is found at some distance away from the centerline. In fact Harvey[8] found it to occur quite near the

boundary. Thus, it would seem that it is not the swirl angle itself which is important, but rather the combined rotational and axial gross characteristics.

The maximum swirl angle, like the onset of surging itself, is more likely a dependent quantity governed by the particular combination of angular-momentum flux, discharge, and draft-tube diameter. However, this assumes that regardless of how angular momemtum is introduced into the draft tube only one unique flow pattern will develop for each value of $\Omega D/\rho Q^2$ In this study, angular momentum was introduced in only one manner--the wicket gates--and, hence, that assumption was not verified or disproved. However, sharp-edged and bell-mouth entrances were used on the 0.286-foot-diameter tube. Equal-length tubes were found to have the same dimensionless frequency and pressure characteristics regardless of entrance condition.

The onset of surging took place in an interesting chain of events. Figure (5a) shows the flow pattern during steady rotating flow. As the wicket gates were closed, increasing the angular-momentum flux in the tube, a zone of reverse flow eventually formed in the jet downstream from the tube. Further increase in $\Omega D/\rho Q^2$ served to move the zone of reversed flow into the tube and upstream along the centerline. Figure (5b) shows the more or less spherical pattern marking the stagnation point which occurs at the upstream end of the reversed-flow zone. Downstream from the spherical pattern the helical-spiral vortex can be seen in Figure (5b). Further closure of the wicket gates moved the centerline stagnation point to the upstream limit of the tube and produced a helical-spiral vortex throughout the length of the tube as shown in Figure (6a). Diffusion of the smoke by turbulence made it impossible to visualize the flow pattern near the downstream end once surging was established throughout the tube.

Two critical values of $\Omega D/\rho Q^2$ were recorded for each tube, one for the value at which reversal occurred at the downstream end of the tube and one corresponding to fully developed surging throughout the tube. For the case of the jet (L/D = 0) there was only one critical value. The spiral vortex observed for the jet is shown in Figure 6(b) while Figure (7b) shows the spiral vortex for fully developed surging in the Fontenelle model draft tube. In the curved draft tube the onset of surging was first observed near the elbow and although smoke patterns never revealed a spiral vortex downstream from the elbow, measurements there did reveal that pressure surging did occur throughout. The critical values of $\Omega D/\rho Q^2$ are shown in Figure (8) along with values obtained by Gore and Ranz[11] and Harvey[8]. For these comparative values it was necessary to assume an axial-velocity distribution in order to compute $\Omega D/\rho Q^2$ since both investigations used swirl angle as the critical parameter. Figure (8) indicates that longer tube lengths produce greater stability against surging.

Figure 8 also indicates that the bend in the draft tube does not influence the breakdown threshold. The divergent cone tested (see Figure 7) had the same expansion rate and same centerline length as the draft tube, but was not bent or deformed. Using centerline length and entrance diameter the L/D ratio of the draft tube and the cone were both 4.77. Expansion of the tube appears to make the flow only slightly less stable against breakdown. The effect of expansion appears reasonable because the local value of $\Omega D/\rho Q^2$ increases as D increases while Ω,p, and Q must remain constant.

Smoke visualization of the helical vortex showed a much more distinct, well defined spiral for both the draft tube and the cone than for the straight tubes (see Figure 7). However, the vortex could not pass through the draft tube bend and was always broken up and diffused at the bend.

C. FREQUENCY AND PRESSURE CHARACTERISTICS

Dimensionless characteristics of pressure and frequency are shown respectively in Figures 13 and 14 in composite for all tubes tested. The values shown were all computed from runs made at Reynolds numbers well beyond 80,000 and therefore do not reflect viscous effects. All experimental points are at values of $\Omega D/\rho Q^2$ above the critical because the pressure-surge signal was difficult to filter out of turbulent noise at low surge amplitudes.

As can be seen, both amplitude and frequency of the surge become smaller as the pipe is made longer, all other variables being held constant. Although pressure variation along the tube was not recorded, it was

[11] Gore, R. W., and W. E. Ranz, "Backflows in Rotating Fluids Moving Axially Through Expanding Cross-Sections," AIChE JOURNAL, January 1964.

observed that the frequency of the surge was constant all along the tube. However the peak-to-peak value of the pressure surge varied along the length of the tube being greatest near the exit of the tube and lowest at the inlet end.

When surging occurred within the exit tube, a pressure fluctuation of equal frequency was observed upstream from the wicket gates inside the stilling chamber. In most cases the amplitude of this upstream pressure fluctuation was at least a factor of five smaller than that observed at the draft tube throat. However, when the surge frequency was near the natural frequency of the system, the amplitude of the pressure fluctuation within the box increased significantly. Natural frequencies of the system (stilling chamber and exit tube) were determined by two different methods. The first method, suggested by Rayleigh, involved observing the frequency of the fluctuations produced by blowing compressed air across the exit opening of the draft tube.[12] In the second method, a loud speaker was driven at successively different frequencies and the pressure response of the system was observed.

The following table shows the natural frequencies of the system as they were determined experimentally. The natural frequencies were substantially different from the frequency of the surge for nearly all recorded measurements. Therefore, it is improbable that the natural frequency had any effect upon the measured surge amplitude or frequency.

TUBE DESCRIPTION		NATURAL FREQUENCY OF SYSTEM
D (ft.)	L/D	f_n (cps)
0.511	3.26	230
0.511	1.63	230
0.511	0	8
0.286	7.20	250

Using the hot-film anemometer to monitor velocity near the tube wall provided a verification that the pressure surge was indeed produced by the precessing helical vortex. Figure 9 shows that the velocity near the piezometer and the pressure signal have the same frequency. (This is an important feature because it clearly shows the connection between the pressure surge and the vortex.)

APPLICATION TO HYDRAULIC TURBINES

The experimental results of this study can be used to investigate the surging potential of hydraulic turbines. Since the parameter $\Omega D/\rho Q^2$ indicates the probability of surging as well as the resulting frequency and pressure-fluctuation amplitude, analysis of a turbine must be directed toward the determination of this parameter.

A. ANALYSIS

In flow through a hydraulic-turbine runner, angular momentum is imparted to the flow as it passes through the wicket gates. As the flow then passes through the turbine runner an exchange of angular momentum is made between the flow and the runner resulting in a net torque on the runner. The torque is equal to the change in the rate of flow of angular momentum produced as the flow passes from the inlet to the outlet of the runner. Figure 15 is a simplified schematic diagram for flow through a runner. The equation for the torque on the runner is

$$T = \Omega_1 - \Omega_2 \tag{7}$$

where $\Omega_1 - \Omega_2$ is the rate of change of angular momentum occurring between points 1 and 2, respectively, the entrance to and exit from the runner. Power delivered by the runner is equal to torque multiplied by ω the angular velocity of the runner. Thus,

$$\frac{P}{\omega} = \Omega_1 - \Omega_2 \tag{8}$$

Multiplication of both sides of Equation (8) by $D/\rho Q^2$ and subsequent rearrangement yields

$$\frac{\Omega_2 D}{\rho Q^2} = \frac{\Omega_1 D}{\rho Q^2} - \frac{PD}{\rho \omega Q^2} \tag{9}$$

[12] Rayleigh, Lord, "Theory of Sound," Dover Press, 1963.

which by incorporation of Equation (6) can be written as

$$\frac{\Omega_2 D}{\rho Q^2} = \frac{D \tan \alpha_1}{2\pi B} - \frac{PD}{\rho\omega Q^2} \qquad (10)$$

The left side of Equation (10) is the momentum parameter of Equations (3) and (5) for the draft tube. On the right side of Equation (10) the first term is the momentum parameter for the flow entering the runner and can be determined if the inlet geometry of the turbine is known. The second term can be determined if the performance characteristics of the turbine are known.

Equation (10) can be used to determine the operating conditions under which the momentum parameter $\Omega_2 D/\rho Q^2$ for the draft tube exceeds the critical value as given in Figure 8. If load and discharge on the turbine are such that flow leaves the runner with no swirl then Ω_2 will be zero, as will $\Omega_2 D/\rho Q^2$, and no surging could occur. The sketch in Figure (20) shows the velocity diagram for flow from the discharge side of a runner blade. The absolute velocity V_2 is determined by the two components: the runner velocity $r_2\omega$ and V_r the velocity of the water relative to the blade. The runner velocity $r_2\omega$ is constant on a speed-regulated unit. However, any change in Q produces a change in V_r. If Q is decreased V_r decreases and V_2 develops a peripheral component in the direction of turbine rotation. If Q is increased, V_r increases and V_2 develops a peripheral component in the direction opposite to turbine rotation. The change in V_r can be caused by either a change in gate opening or a change in head. If swirl occurs in the direction of the runner, Ω_2 in Equation (10), and hence $\Omega_2 D/\rho Q^2$ as well, will be positive. For swirl in the direction opposite to the runner, the sign of $\Omega_2 D/\rho Q^2$ will be negative. Surging is independent of swirl direction and, thus, it is the absolute value of $\Omega_2 D/\rho Q^2$ which is of importance.

Equation (10) was used to analyze model-performance data for the Fontenelle and Hoover-replacement runners. Figure (16) shows the $\Omega D/\rho Q^2$ and efficiency characteristics for the Fontenelle model as a function of standard unit parameters. For operation within the $\Omega D/\rho Q^2 = 0.4$ contour surging should not be expected. However, operation outside of that contour should produce surging. Note that the region of maximum efficiency lies within the smooth operation region, but that rough operation could conceivably occur at a discharge only slightly larger than that realized at maximum efficiency (assuming constant head). Contours of large $\Omega D/\rho Q^2$ will indicate regions of relatively high frequency and pressure-fluctuation amplitude.

Upward and to the left of the dashed line in Figure (16) the flow in the draft tube whirls in the same direction as the runner while below and to the right of the line the whirl is opposite to the runner. Power swings observed on the Fontenelle prototype are plotted on Figure (16) in megawatts. Because the interaction between turbine and power system is not known, little can be said about the power swings except that they are in general agreement with predicted regions of surging.

Analysis of the Hoover model data produced the plot of characteristics shown in Figure (17). Again a region of surge-free operation is predicted. The manufacturer of the Hoover model did not provide as large a range of performance data as was available for the Fontenelle model. However, the water leaving the wicket gates does not necessarily leave tangent to the gate. Experience with the Hoover data showed that the method used in determining $\Omega_1 D/\rho Q^2$ for use in Equation (9) needs further investigation. Using D tan $\alpha_1/2\pi B$ may produce an $\Omega_2 D/\rho Q^2$ which is incorrect.

B. EFFECT OF TAILWATER

In prototype plants it has been noted that increasing tailwater depth generally results in stronger pressure surges while decreasing the depth seems to alleviate the surging. In the air model such a phenomenon could not be observed because an increase in pressure at the outlet end would simply increase the pressure throughout the system and decrease the discharge for a given gate opening. This, according to the results of this study summarized in Figures (13) and (14), would not change $\Omega D/\rho Q^2$ and would, hence, not change the frequency or pressure parameter.

One must conclude, therefore, that the tailwater effect is a condition involving two-phase flow. If the tailwater depth is reduced the pressure in the draft tube is reduced and water vapor may be created and fill the core or air may be drawn in through existing aeration devices and then may replace the core of the vortex in the draft tube. At high tailwater cavitation may be eliminated and because of increased draft-tube pressure air may not be drawn into the draft tube. Under these conditions the core will fill with water and the surge is dynamically similar to the air model observed in this study. Air injection is known to alleviate surging which agrees with the above reasoning.[12] The air or vapor-filled core has been observed by many investigators.[2,3,12] With the vortex core filled with air or vapor the mass of fluid oscillating in the draft tube is reduced and thus one would expect the pressure amplitudes to be reduced even though the surge frequency may possibly remain the same.

Figure (18) shows a dimensionless plot of surge frequency parameter versus $\Omega D/\rho Q^2$ for various values of σ for the Hoover model (σ is the cavitation number for the turbine).

Figure (19) shows a corresponding plot of the pressure parameter. The plots indicate that both frequency and pressure decrease as σ is decreased. At σ = 0.30 the frequency parameters and pressure parameters are in reasonable agreement with those of this study for corresponding values of $\Omega D/\rho Q^2$.

MODEL-PROTOTYPE SIMILITUDE

Equations (3) and (5) express functionally the relationships of interest in applying the experimental results of this study to a prototype turbine draft tube.

$$\frac{fD^3}{Q} = \phi_1\left(\frac{\Omega D}{\rho Q^2}, \frac{L}{D}, R\right) \qquad (3)$$

$$\frac{\Delta P D^3}{\Omega} = \phi_2\left(\frac{\Omega D}{\rho Q^2}, \frac{L}{D}, R\right) \qquad (5)$$

Using subscripts of M and P to represent model and prototype, respectively, the conditions of dynamic and geometric similitude are

$$\left(\frac{\Omega D}{\rho Q^2}\right)_M = \left(\frac{\Omega D}{\rho Q^2}\right)_p \qquad \left(\frac{L}{D}\right)_M = \frac{L}{D}\Big)_P \qquad (11)$$

For viscous similarity all that is required is that the Reynolds number of the prototype be at least equal to 80,000.

If the similitude relationships of Equations (11) are satisfied it follows from Equations (3) and (5) that

$$\left(\frac{fD^3}{Q}\right)_M = \left(\frac{fD^3}{Q}\right)_P \qquad \left(\frac{\Delta P D^3}{\Omega}\right)_M = \left(\frac{\Delta P D^3}{\Omega}\right)_P \qquad (12)$$

Thus, the prototype surge amplitude will be

$$\Delta P_p = \Delta P_M \left(\frac{D_M}{D_P}\right)^3 \left(\frac{\Omega_P}{\Omega_M}\right) \qquad (13)$$

Using the first of the similitude relations in Equation (11)

$$\Delta P_p = \left(\frac{\Delta P D^3}{\Omega}\right)_M \left(\frac{\Omega D}{\rho Q^2}\right)_M \left(\frac{\rho Q^2}{D^4}\right)_P \qquad (14)$$

similarly, the prototype surge frequency will be

$$f_P = f_m \left(\frac{D_m}{D_p}\right)^3 \frac{Q_p}{Q_m} \qquad (15)$$

If information on the model is known in terms of $\Omega D/\rho Q^2$ Equations (14) and (15) can be used to determine frequency and magnitude of pressure surging for the prototype. Predicted pressure may, however, be altered by plant σ and by possible resonance in the system.

(Example)

For Fontenelle turbine and draft tube

Dp = 10.00′ (3.048 m), ρ_p = 1.94 slugs/ft^3 (1.0 gm/cm^3)

Picking a point on Figure (16) where $\Omega D/\rho Q^2 = 1.00$,

$Q/D_R^2\sqrt{H} = 1.75$ and $\pi D_R n/60\sqrt{2gH} = 0.80$

Then, because D_{R_p}=7.416′ (2.2606 m) and np=150 rpm, H_P = 83′ (25.2 m) and Q_P = 880 cfs (24.9 m^3/sec).

From Figures (13) and (14) we obtain $\left(\frac{fD^3}{Q}\right)_M = 0.88$ and $\left(\frac{\Delta PD^3}{\Omega}\right)_M = 4.5$

Thus,

$$f_P = \left(\frac{fD^3}{Q}\right)_M \left(\frac{Q}{D^3}\right)_P = 0.88 \left(\frac{880}{1000}\right) = 0.78 \text{ cps}$$

$$\Delta P_P = \left(\frac{\Delta PD^3}{\Omega}\right)_M \left(\frac{\Omega D}{PQ^2}\right)_M \left(\frac{\rho Q^2}{D^4}\right)_P$$

$$= 4.5\ (1.00)\ \frac{1.94\ (880)^2}{(10)^4} = 695 \text{ psf} = 11.1 \text{ ft (3.38 m) water}$$

The rotational speed for Fontenelle is 150 rpm, Rheingans Equation (1) predicts a frequency of 0.63 cps. Thus, the predicted results above appear reasonable.

FIGURE 1
REPORT HYD-591

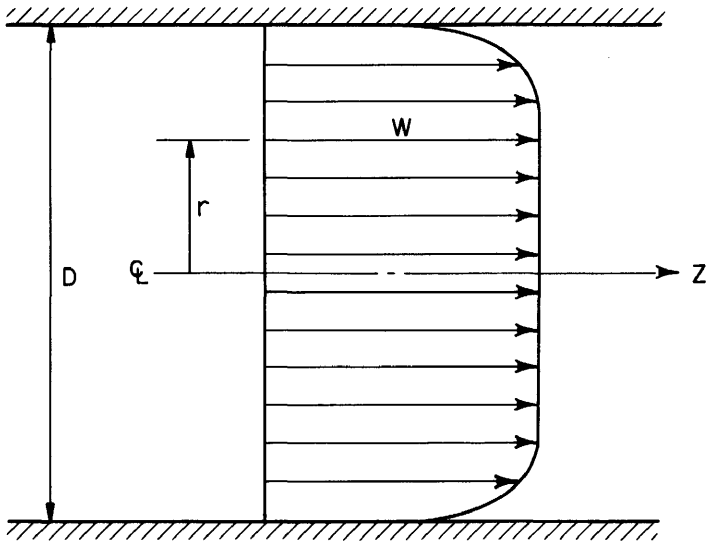

(a) PURELY AXIAL TURBULENT FLOW

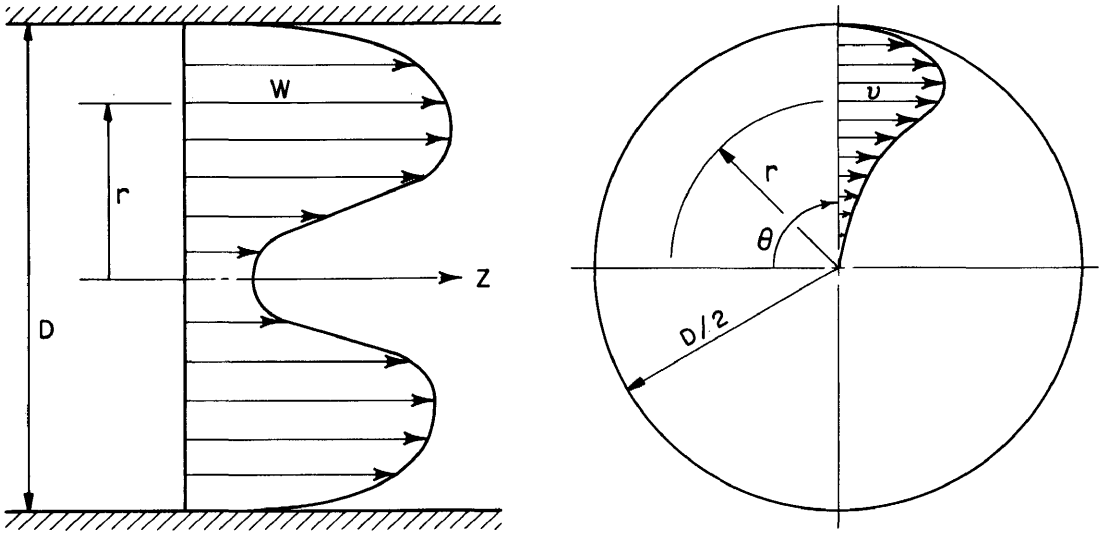

(b) AXIAL FLOW WITH ROTATION

EFFECT OF ROTATION ON FLOW PATTERN

739

A. Overall view from downstream end. Photo PX-D-64111.

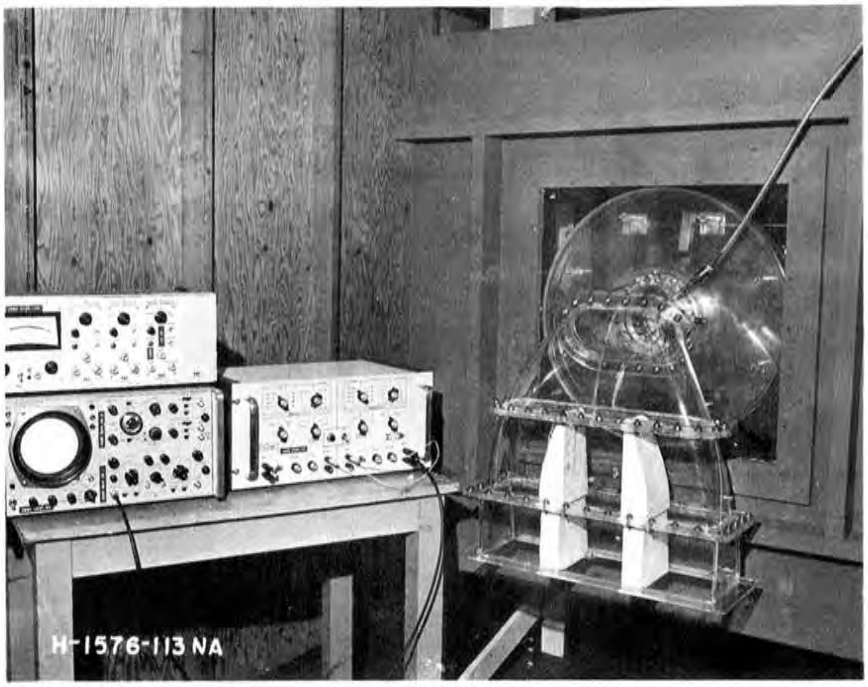

B. View of outlet with model of Fontenelle draft tube mounted. Photo PX-D-64112.

DRAFT–TUBE SURGE STUDY
Experimental Apparatus

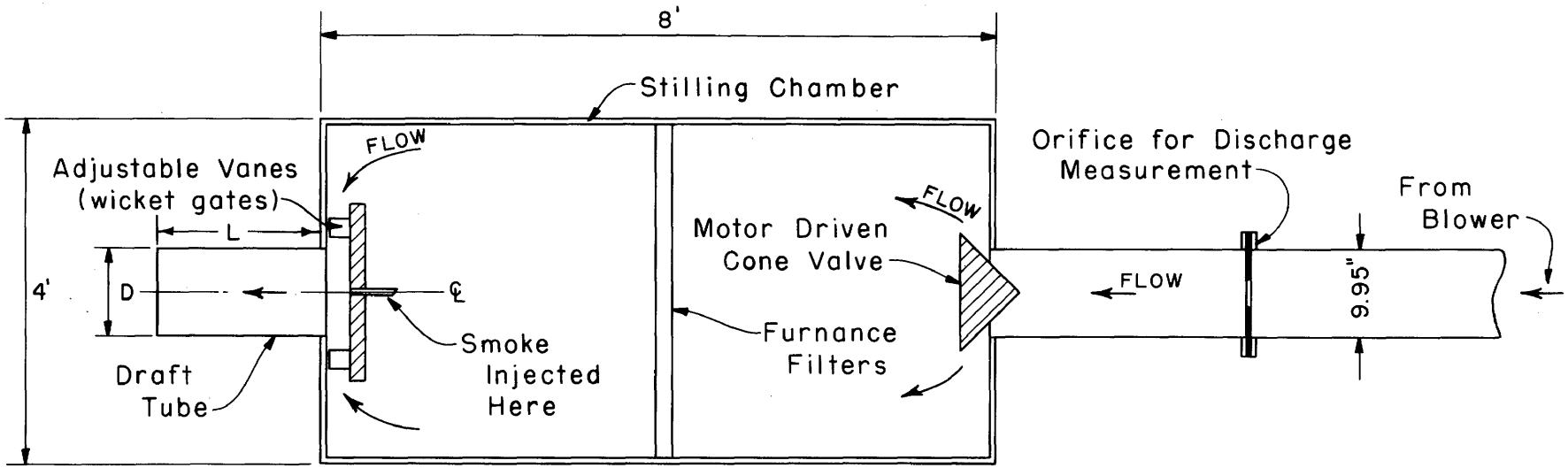

SCHEMATIC DIAGRAM OF APPARATUS

FIGURE 3
REPORT HYD-591

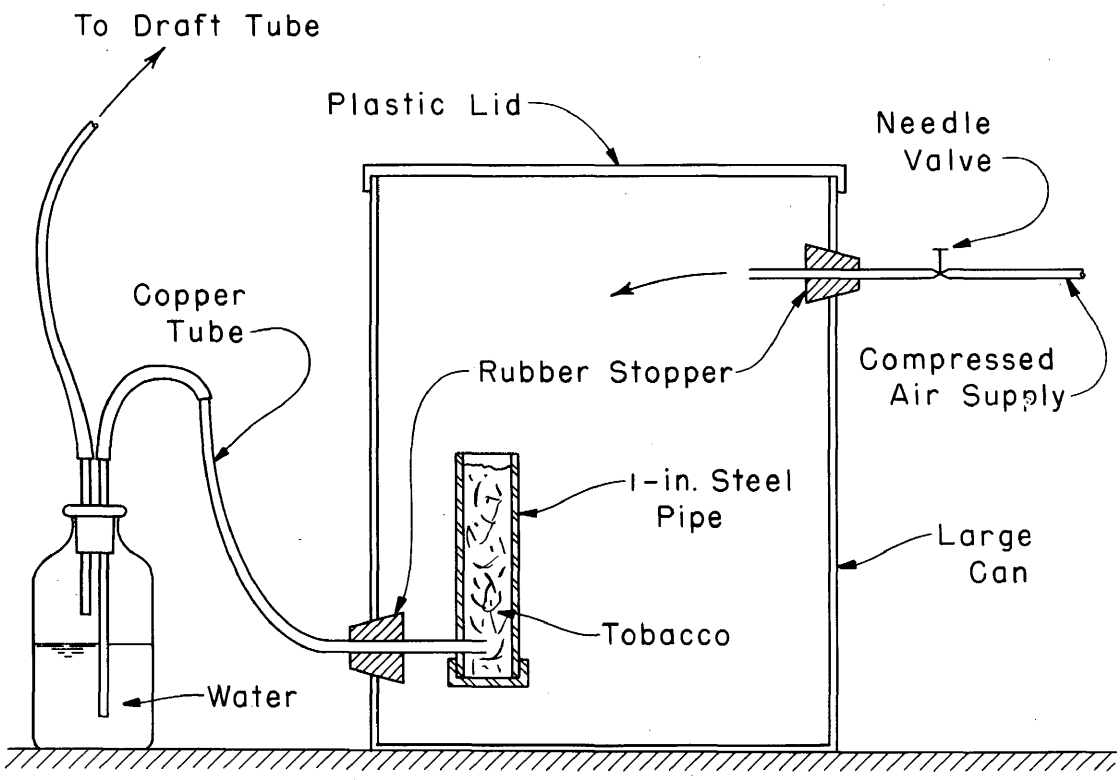

SMOKE GENERATOR

Figure 5
Report HYD-591

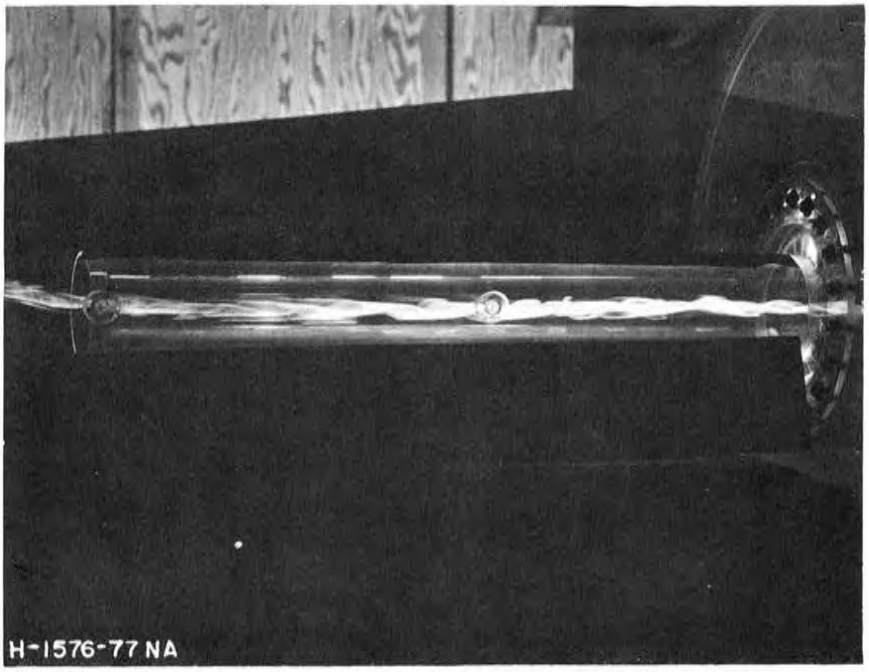

A. Steady uniformly swirling flow
D = 3.44 in. (8.76 cm), $\frac{L}{D}$ = 7.20, $\frac{\Omega D}{\rho Q^2}$ = 0.100

Photo PX-D-64109.

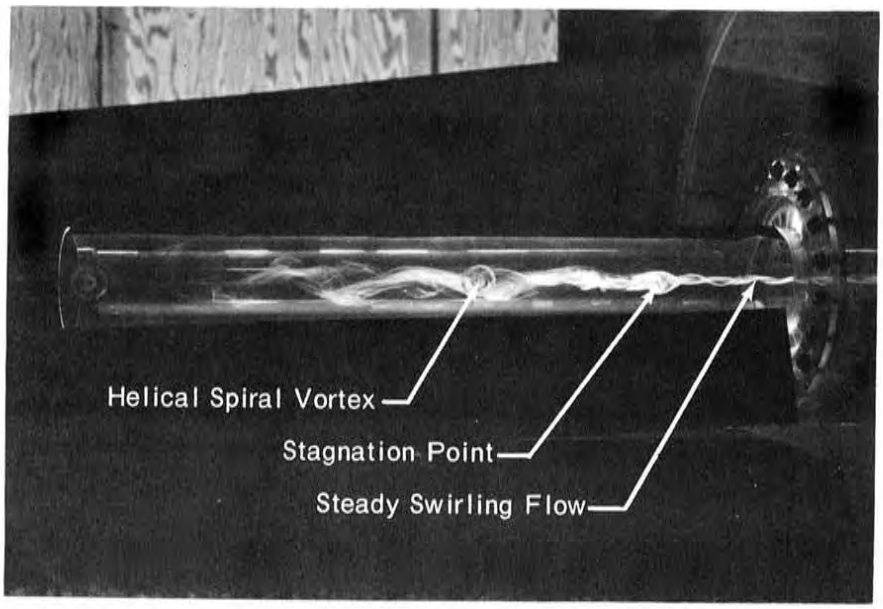

B. Reversal and surging

D = 3.144 in. (8.76 cm), $\frac{L}{D}$ = 7.20 $\frac{\Omega D}{\rho Q^2}$ = 0.280

Photo PX-D-64110.

Figure 6
Report HYD-591

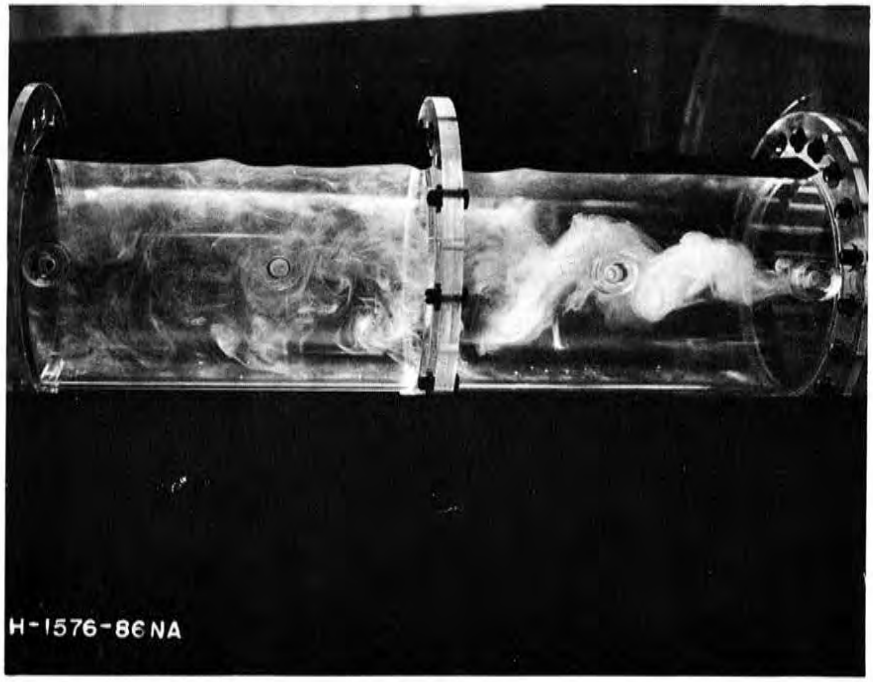

A. Fully established surging

D = 6.13 in. (15.56 cm), $\frac{L}{D}$ = 3.26, $\frac{\Omega D}{\rho Q^2}$ = 0.354

Photo PX-D-64107

B. Surging in an open jet

D = 6.13 in. (15.56 cm), $\frac{L}{D}$ = 0.0, $\frac{\Omega D}{\rho Q^2}$ = 0.300

Photo PX-D-64108.

DRAFT-TUBE SURGE STUDY
Photographs of Flow Patterns

Figure 7
Report HYD-591

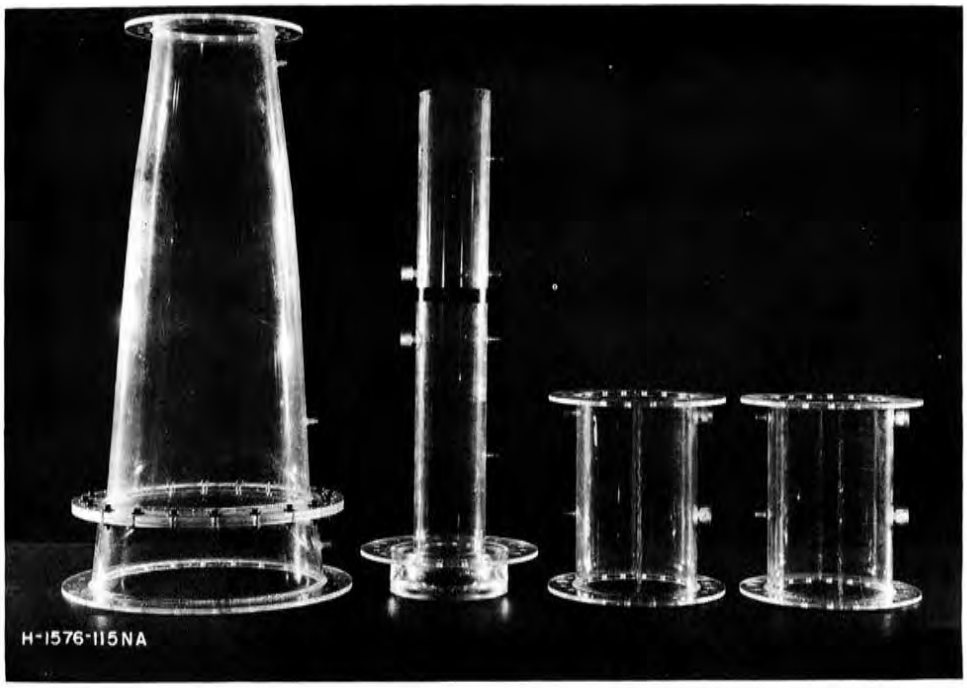

A. Draft tubes that were tested. Photo PX-D-64105.

B. Fully established surging in the model of the Fontenelle Draft Tube.

D = 6.13 in. (15.56 cm), $\frac{L}{D}$ = 4.77, $\frac{\Omega D}{\rho Q^2}$ = 0.400

Photo PX-D-64106.

DRAFT-TUBE SURGE STUDY
Draft Tubes and Flow Patterns

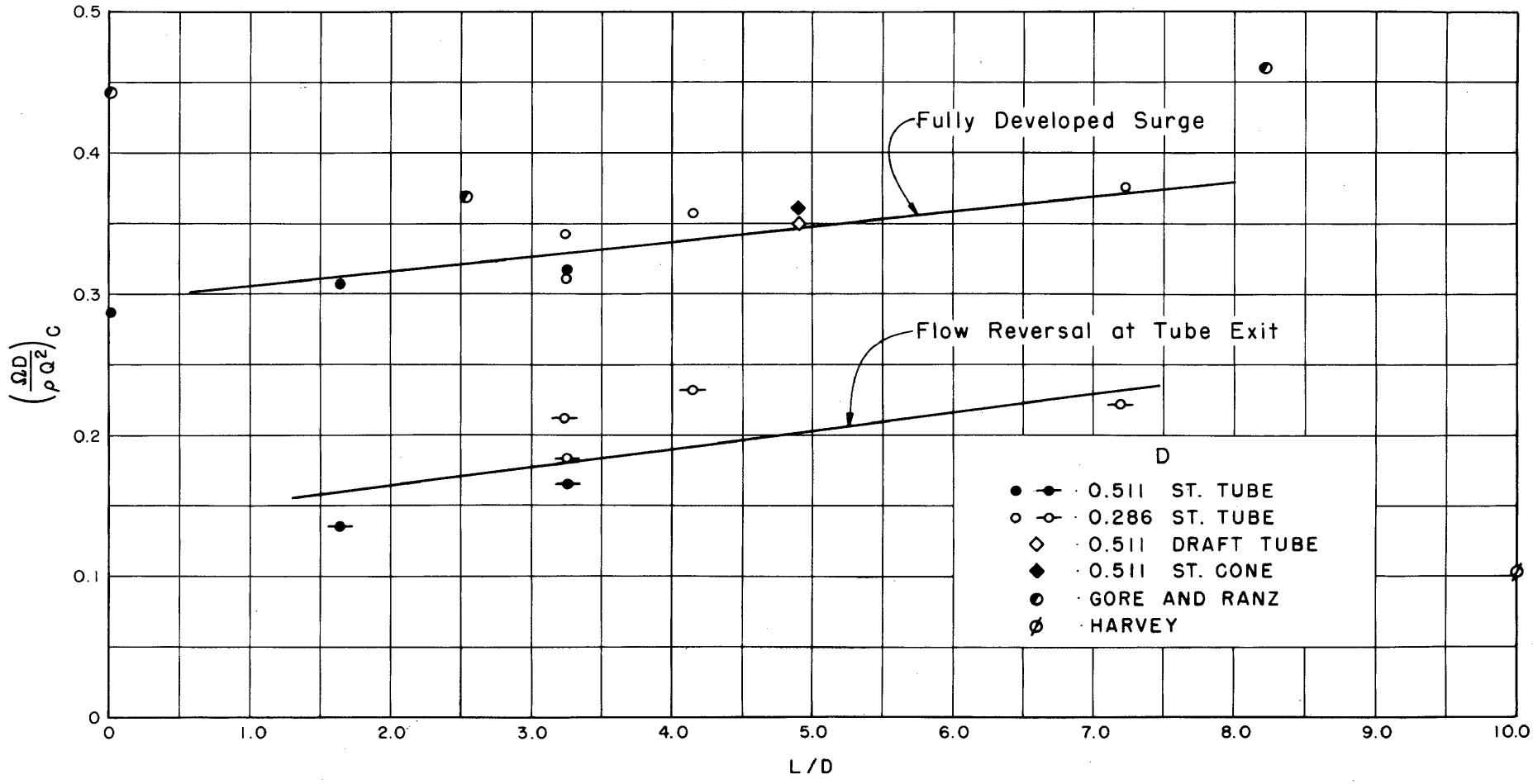

CRITICAL VALUES OF $\Omega D/\rho Q^2$

FIGURE 8
REPORT HYD-591

Figure 9
Report HYD-591

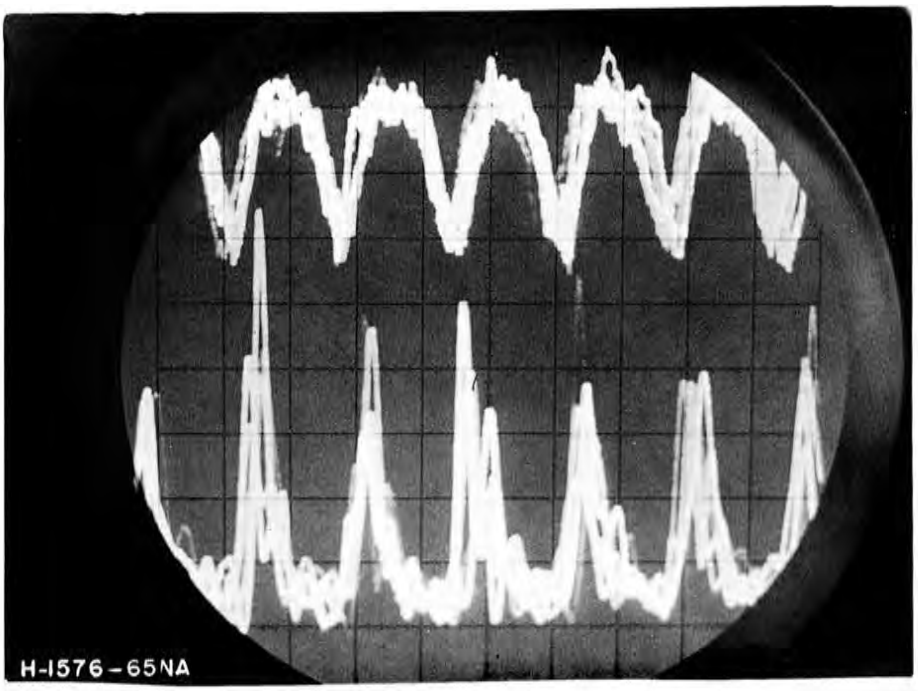

Velocity (upper) and pressure (lower) traces photographed on the oscilloscope

$D = 6.13$ in. (15.56 cm), $\frac{L}{D} = 1.63$, $\frac{\Omega D}{\rho Q^2} = 1.000$

Photo PX-D-64104.

DRAFT-TUBE SURGE STUDY

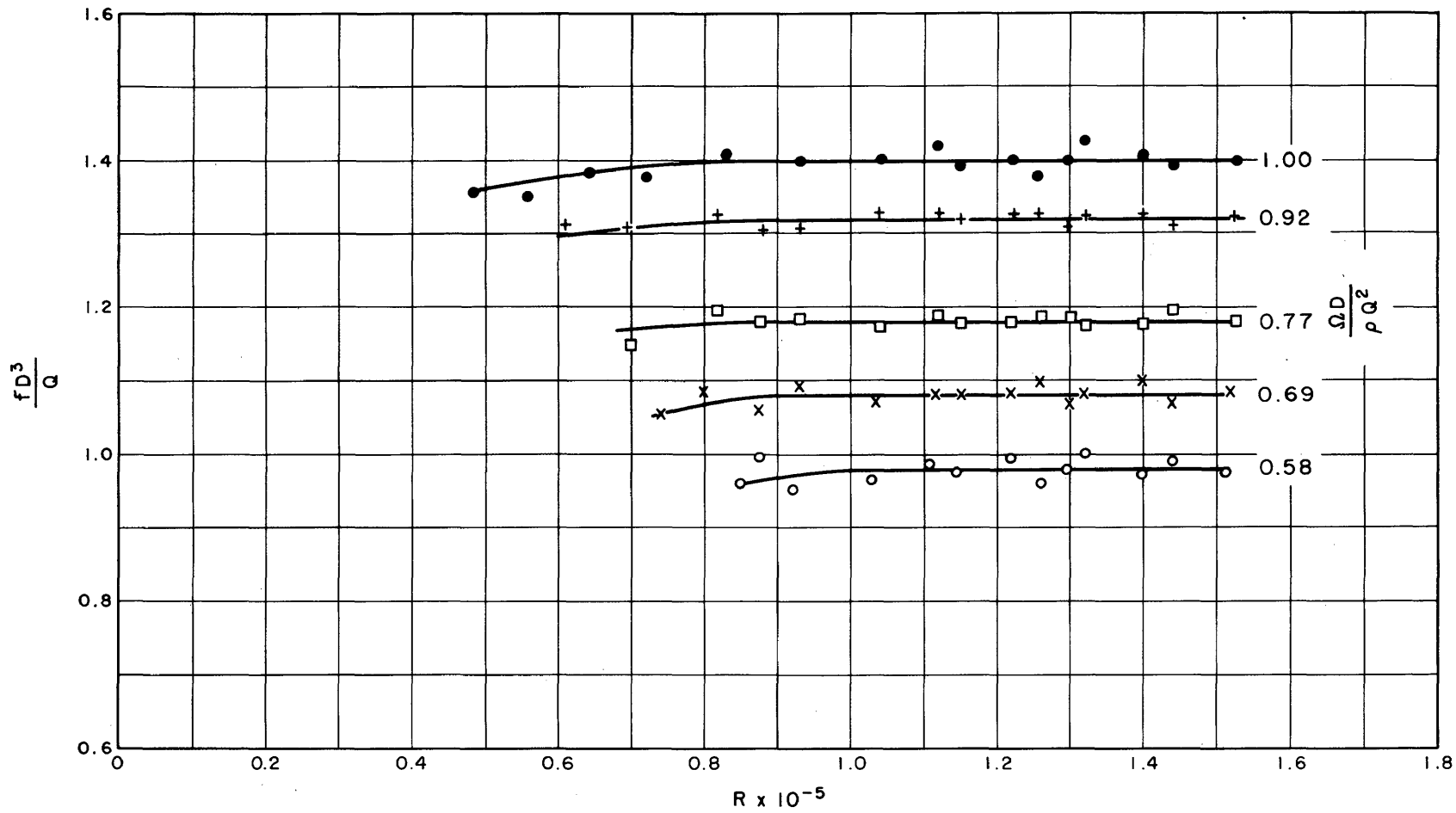

FREQUENCY PARAMETER AS A FUNCTION OF REYNOLDS NUMBER FOR STRAIGHT TUBES

D = 0.5' (15.26 cm) L/D = 1.63

FIGURE 10
REPORT HYD-591

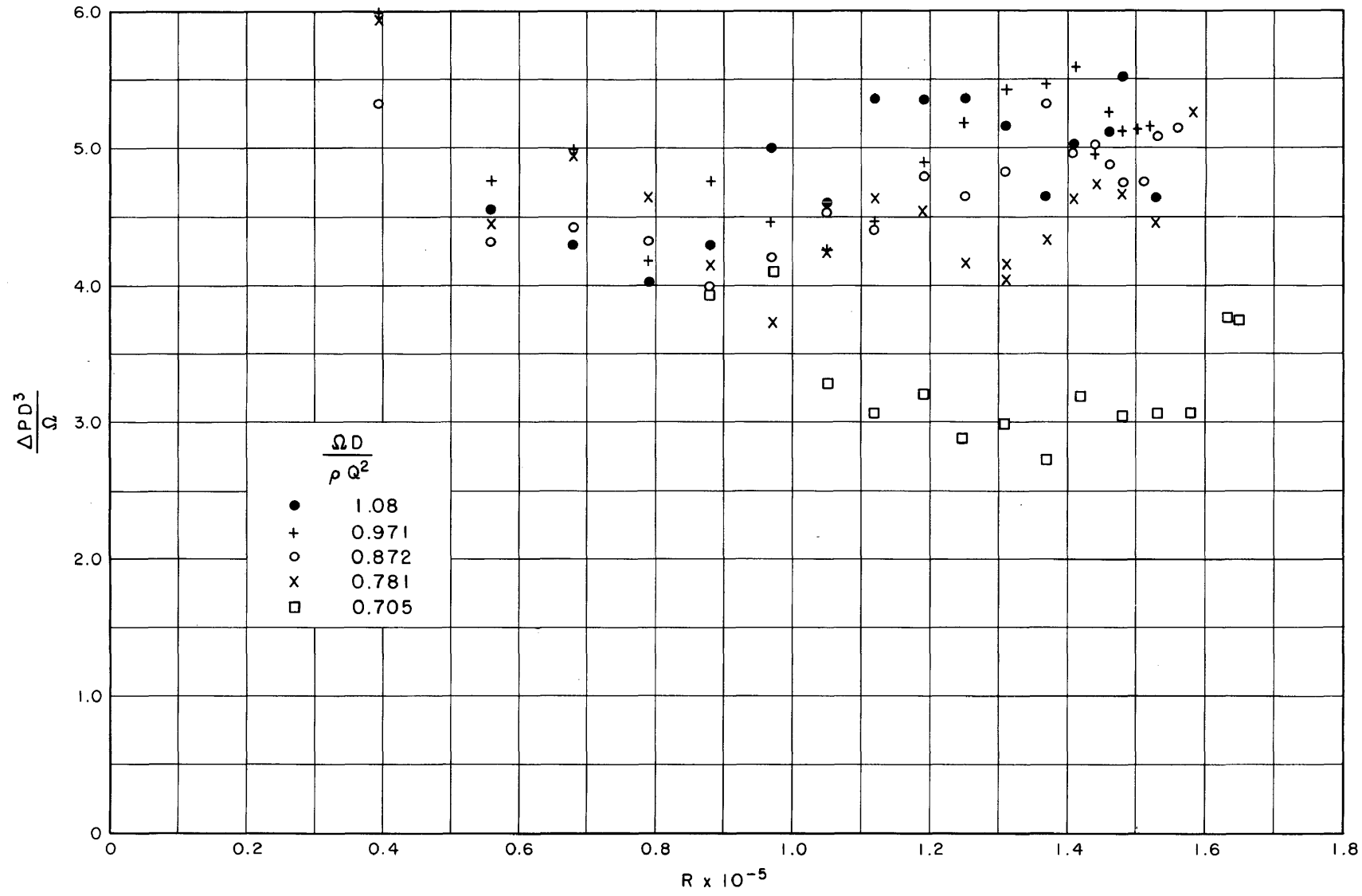

PRESSURE PARAMETER AS A FUNCTION OF REYNOLDS NUMBER, STRAIGHT TUBE
D = 0.5' (15.26 cm) L/D = 4.771

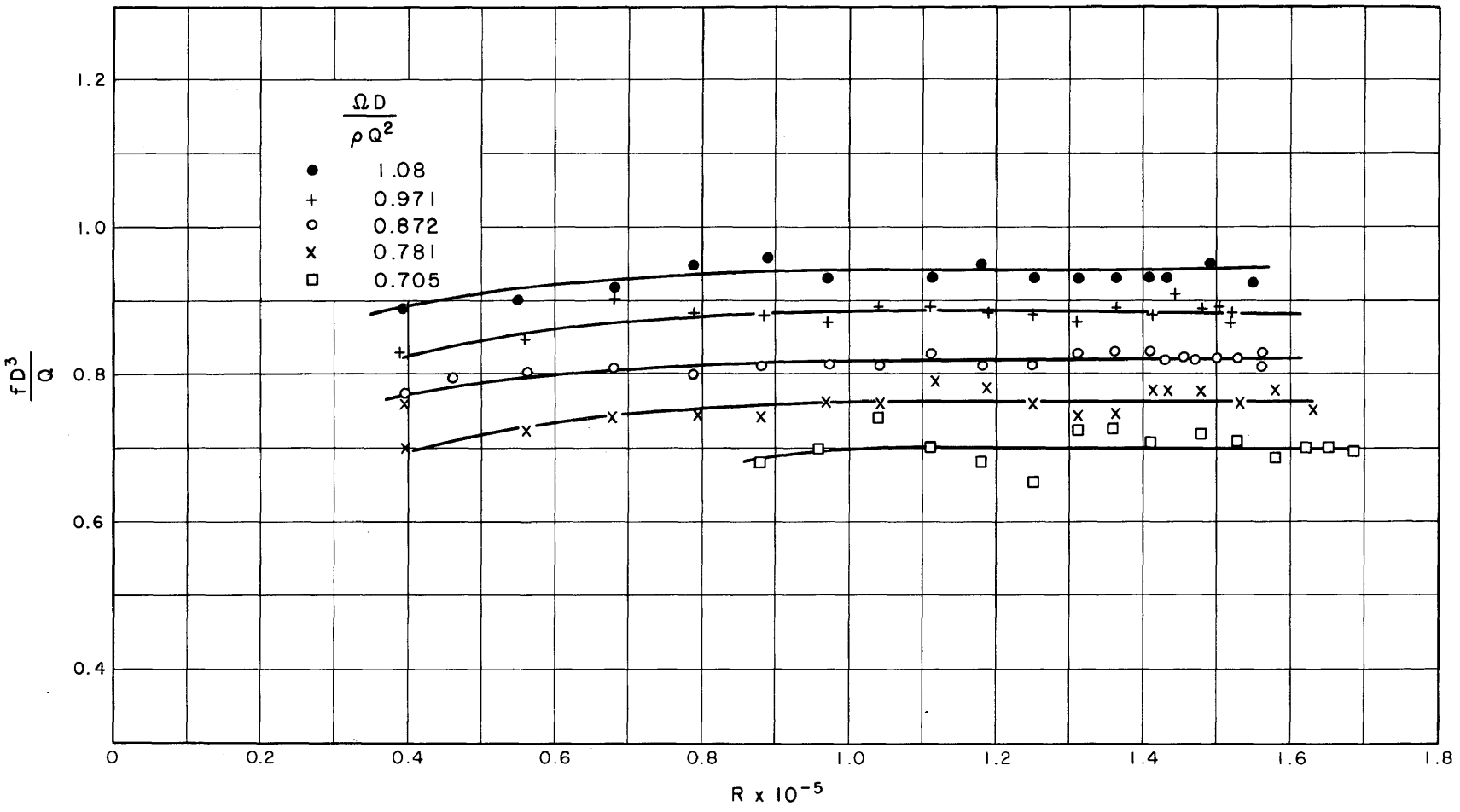

FREQUENCY PARAMETER AS A FUNCTION OF REYNOLDS NUMBER FOR THE FONTENELLE DRAFT TUBE
D = 0.5' (15.26 cm) L/D = 4.77

FIGURE 12
REPORT HYD-591

FIGURE 13
REPORT HYD-591

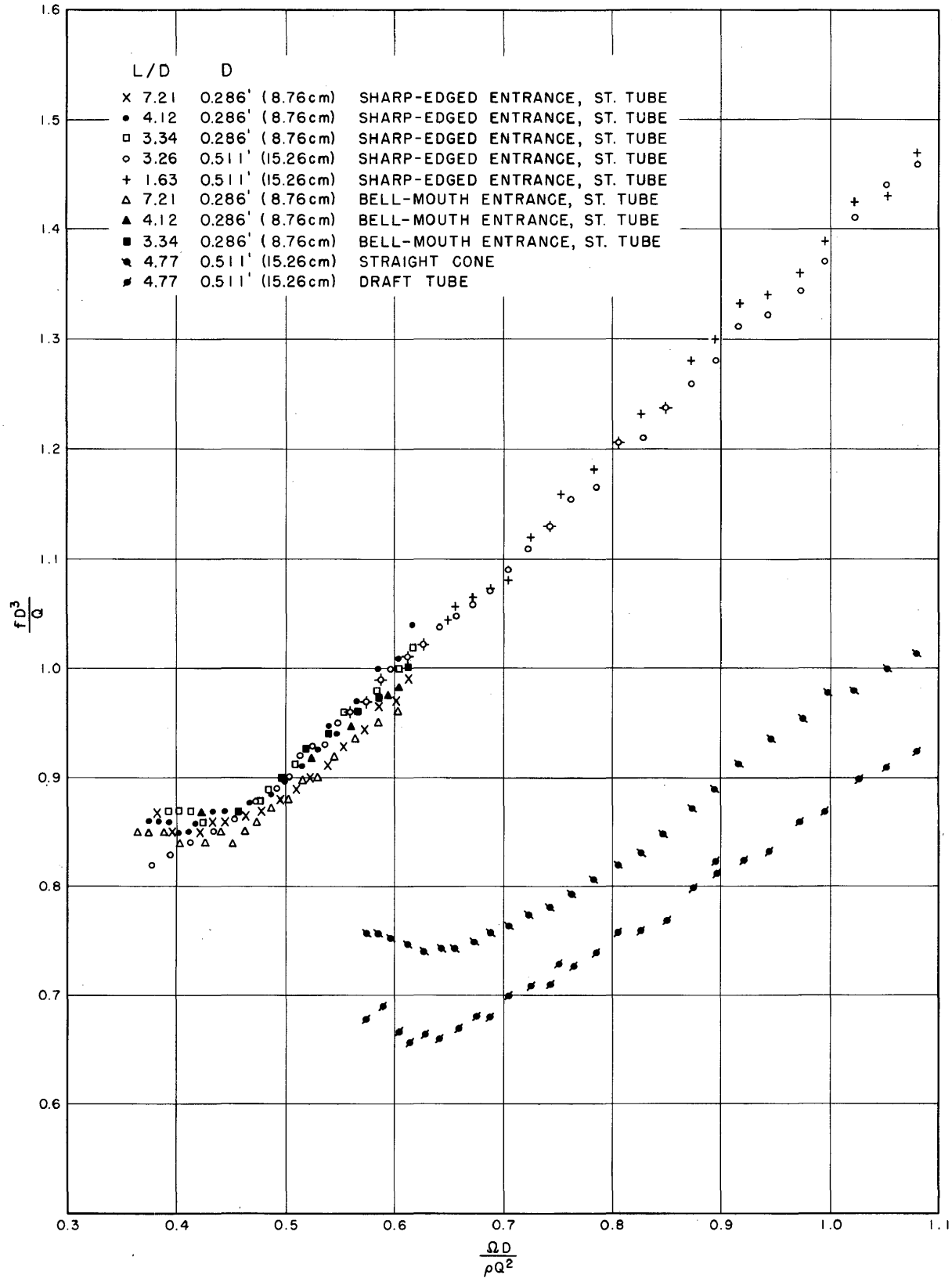

FREQUENCY PARAMETER FOR ALL TUBES AS A FUNCTION OF THE MOMENTUM PARAMETER

739

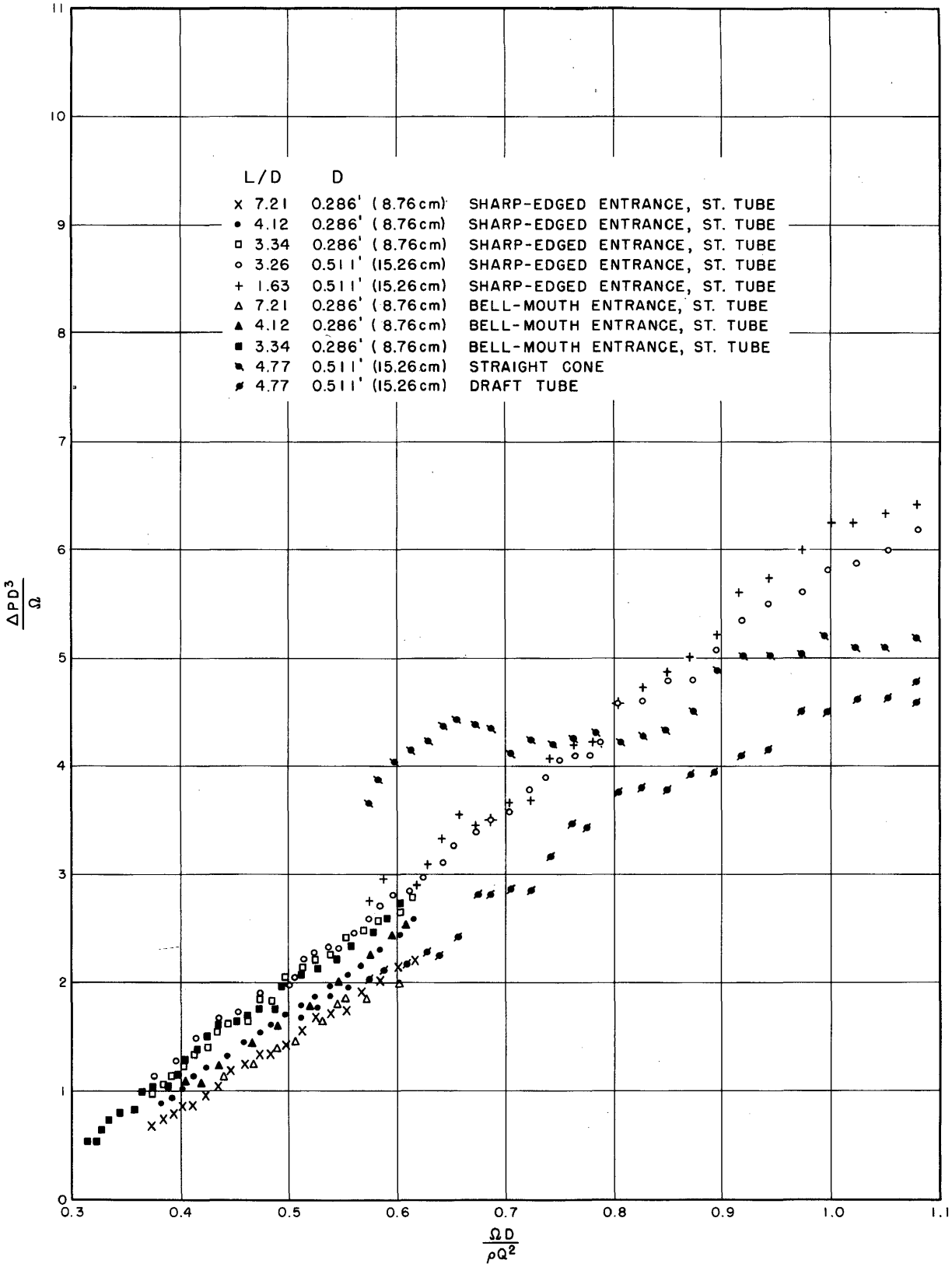

PRESSURE PARAMETER FOR ALL TUBES AS A FUNCTION OF MOMENTUM PARAMETER

FIGURE 15
REPORT HYD-591

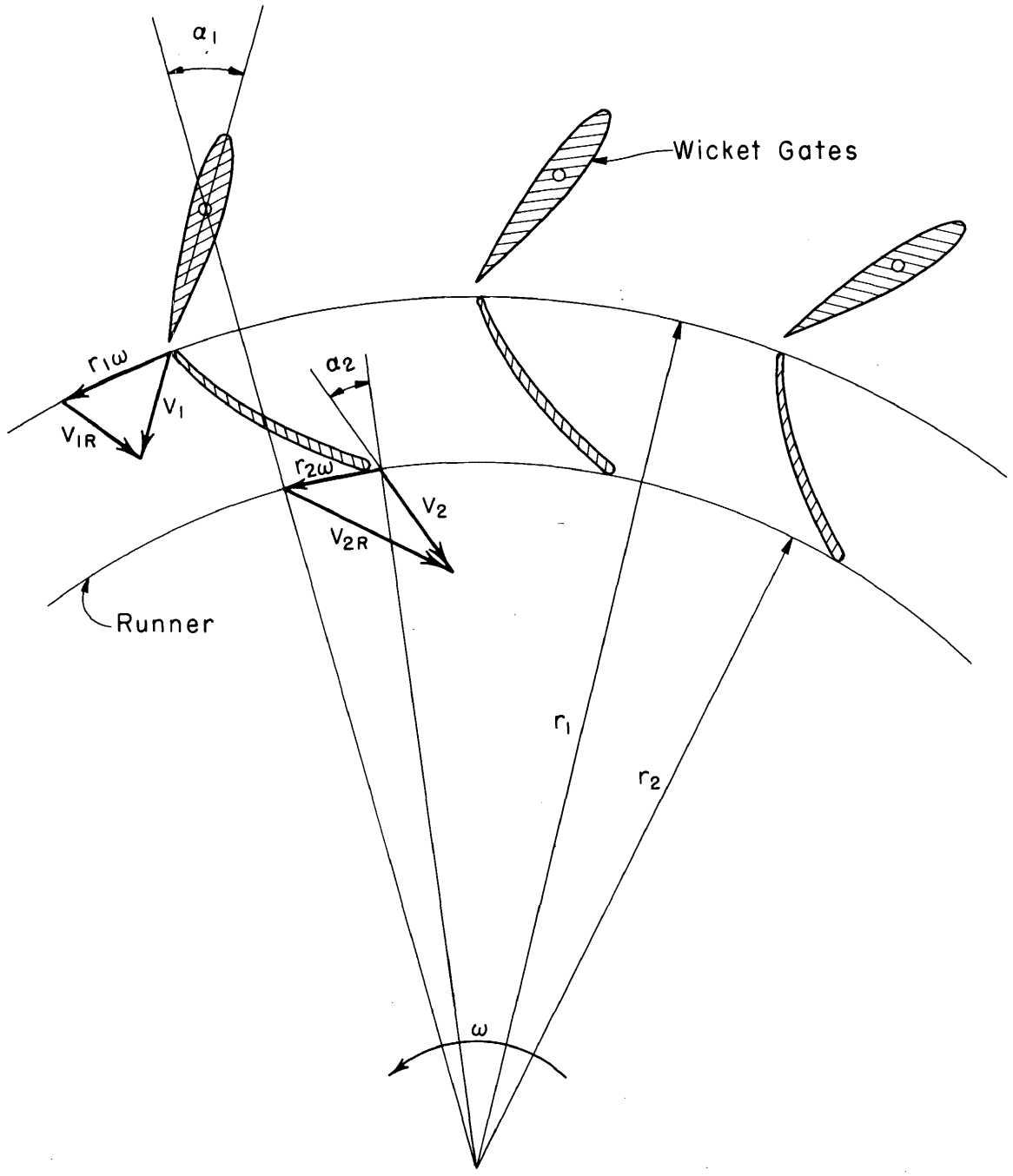

VELOCITY DIAGRAMS FOR A TURBINE RUNNER

739

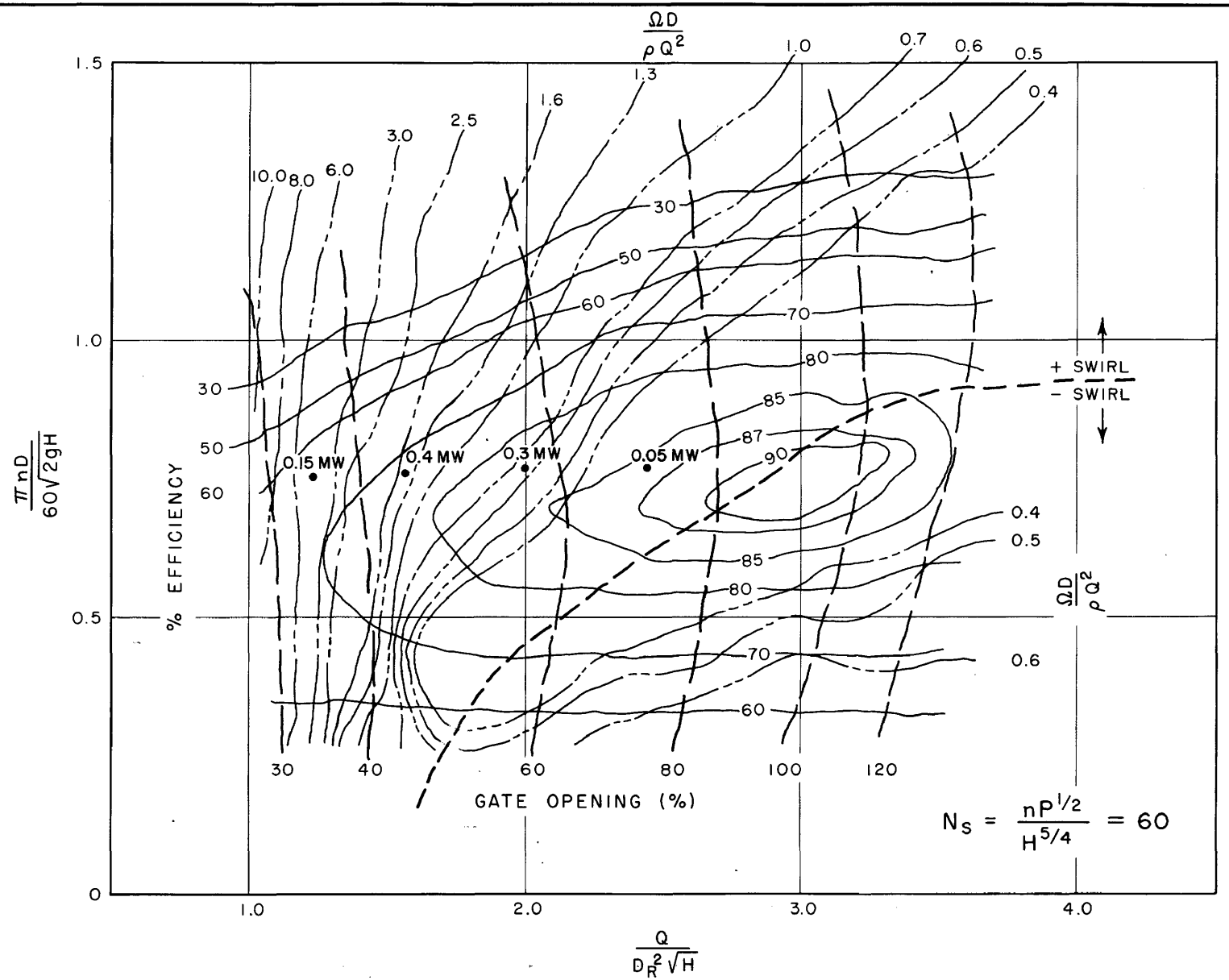

OPERATING CHARACTERISTICS FOR FONTENELLE MODEL TURBINE

FIGURE 16
REPORT HYD-591

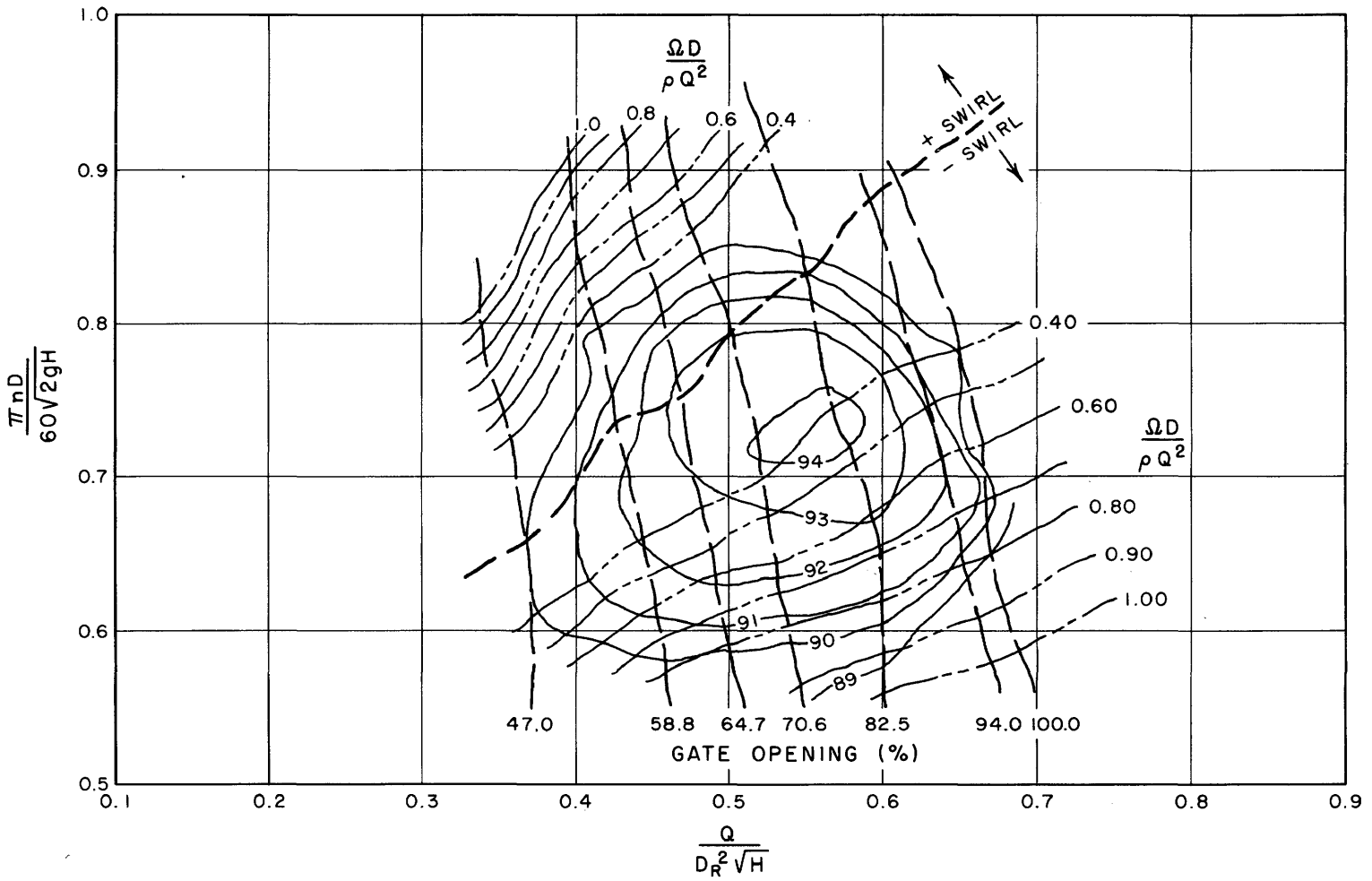

EFFICIENCY HILL - HOOVER REPLACEMENT RUNNER - MODEL DATA

$$N_S = \frac{nP^{1/2}}{H^{5/4}} = 28$$

FIGURE 17
REPORT HYD-591

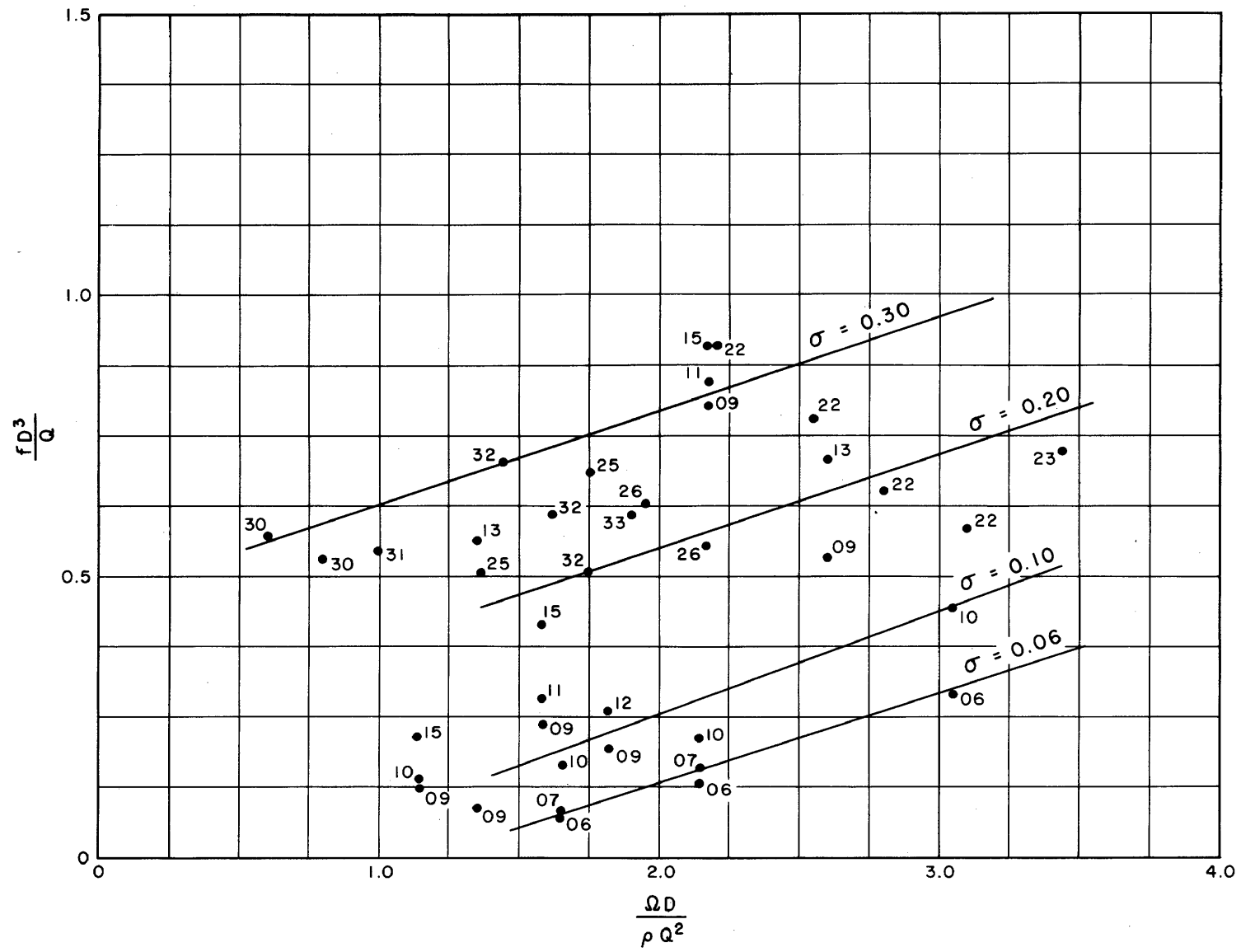

HOOVER MODEL DATA - FREQUENCY, MOMENTUM, σ

FIGURE 18
REPORT HYD-591

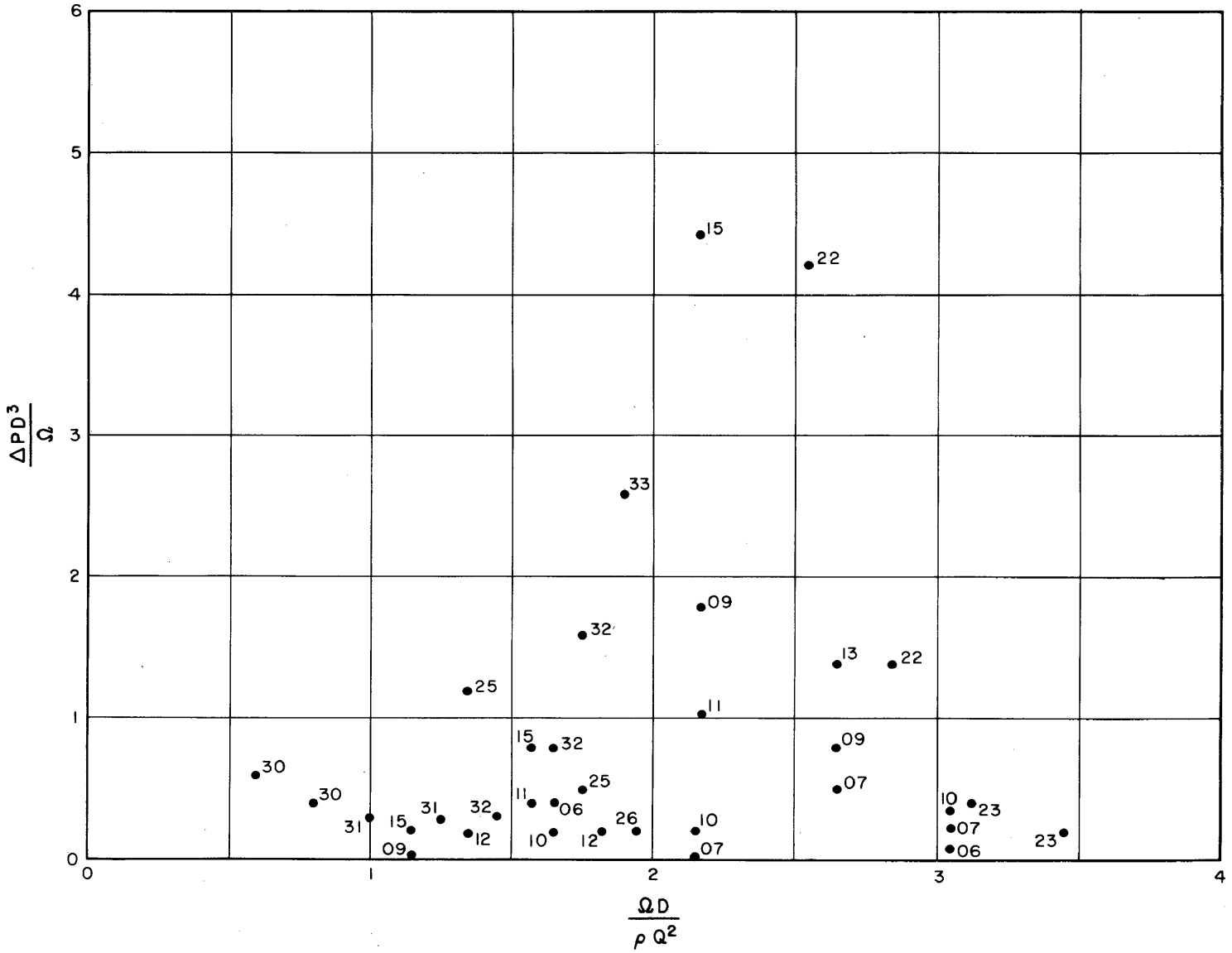

HOOVER REPLACEMENT RUNNER MODEL DATA, PRESSURE PARAMETER VERSUS MOMENTUM PARAMETER FOR VARIOUS VALUES OF σ

FIGURE 19
REPORT HYD-591

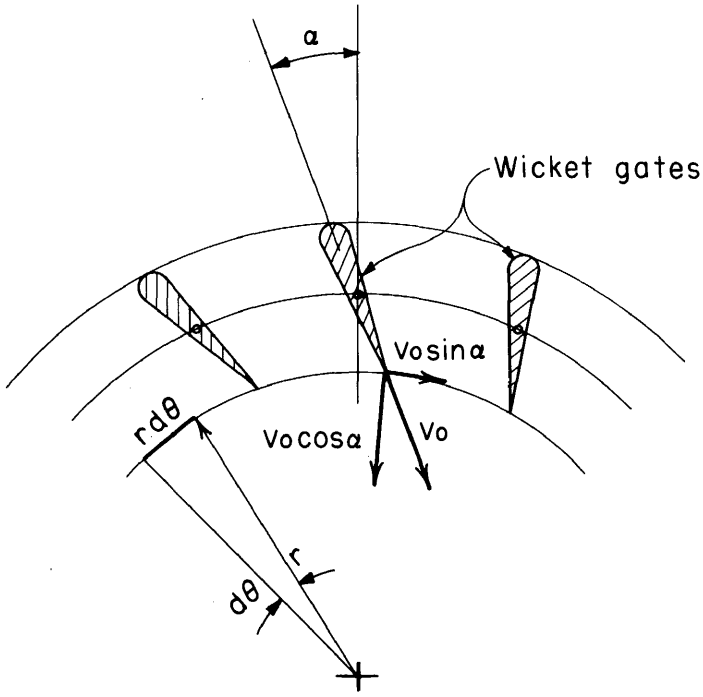

a. FLOW LEAVING WICKET GATES

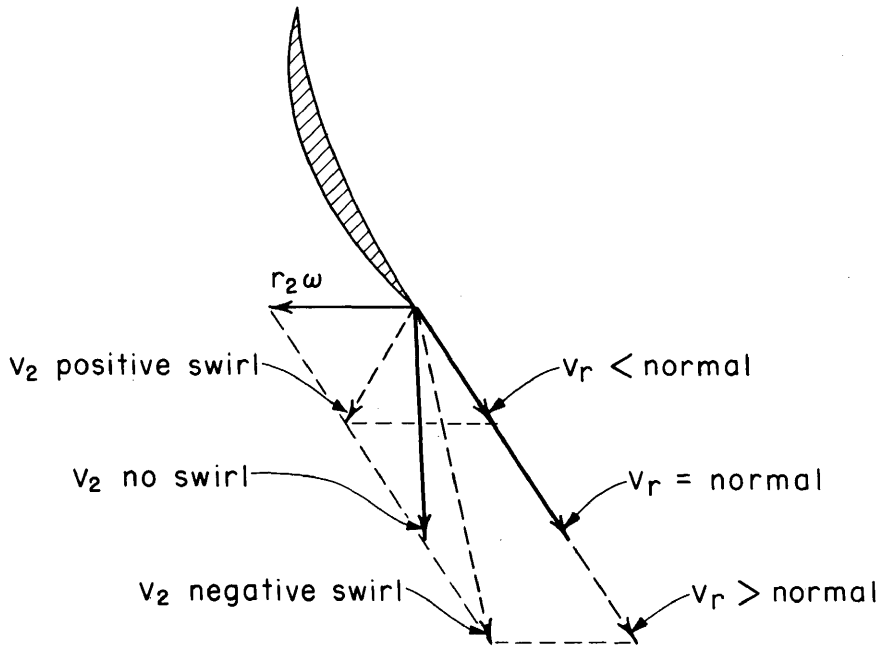

b. FLOW AT EXIT FROM TURBINE RUNNER

FLOW THROUGH A TURBINE

739

7-1750
(2-67)
Bureau of Reclamation

CONVERSION FACTORS--BRITISH TO METRIC UNITS OF MEASUREMENT

The following conversion factors adopted by the Bureau of Reclamation are those published by the American Society for Testing and Materials (ASTM Metric Practice Guide, January 1964) except that additional factors (*) commonly used in the Bureau have been added. Further discussion of definitions of quantities and units is given on pages 10-11 of the ASTM Metric Practice Guide.

The metric units and conversion factors adopted by the ASTM are based on the "International System of Units" (designated SI for Systeme International d'Unites), fixed by the International Committee for Weights and Measures; this system is also known as the Giorgi or MKSA (meter-kilogram (mass)-second-ampere) system. This system has been adopted by the International Organization for Standardization in ISO Recommendation R-31.

The metric technical unit of force is the kilogram-force; this is the force which, when applied to a body having a mass of 1 kg, gives it an acceleration of 9.80665 m/sec/sec, the standard acceleration of free fall toward the earth's center for sea level at 45 deg latitude. The metric unit of force in SI units is the newton (N), which is defined as that force which, when applied to a body having a mass of 1 kg, gives it an acceleration of 1 m/sec/sec. These units must be distinguished from the (inconstant) local weight of a body having a mass of 1 kg; that is, the weight of a body is that force with which a body is attracted to the earth and is equal to the mass of a body multiplied by the acceleration due to gravity. However, because it is general practice to use "pound" rather than the technically correct term "pound-force," the term "kilogram" (or derived mass unit) has been used in this guide instead of "kilogram-force" in expressing the conversion factors for forces. The newton unit of force will find increasing use, and is essential in SI units.

Table I

QUANTITIES AND UNITS OF SPACE

Multiply	By	To obtain
LENGTH		
Mil	25.4 (exactly)	Micron
Inches	25.4 (exactly)	Millimeters
	2.54 (exactly)*	Centimeters
Feet	30.48 (exactly)	Centimeters
	0.3048 (exactly)*	Meters
	0.0003048 (exactly)*	Kilometers
Yards	0.9144 (exactly)	Meters
Miles (statute)	1,609.344 (exactly)*	Meters
	1.609344 (exactly)	Kilometers
AREA		
Square inches	6.4516 (exactly)	Square centimeters
Square feet	929.03*	Square centimeters
	0.092903	Square meters
Square yards	0.836127	Square meters
Acres	0.40469*	Hectares
	4,046.9*	Square meters
	0.0040469*	Square kilometers
Square miles	2.58999	Square kilometers
VOLUME		
Cubic inches	16.3871	Cubic centimeters
Cubic feet	0.0283168	Cubic meters
Cubic yards	0.764555	Cubic meters
CAPACITY		
Fluid ounces (U.S.)	29.5737	Cubic centimeters
	29.5729	Milliliters
Liquid pints (U.S.)	0.473179	Cubic decimeters
	0.473166	Liters
Quarts (U.S.)	946.358*	Cubic centimeters
	0.946331*	Liters
Gallons (U.S.)	3,785.43*	Cubic centimeters
	3.78543	Cubic decimeters
	3.78533	Liters
	0.00378543*	Cubic meters
Gallons (U.K.)	4.54609	Cubic decimeters
	4.54596	Liters
Cubic feet	28.3160	Liters
Cubic yards	764.55*	Liters
Acre-feet	1,233.5*	Cubic meters
	1,233,500*	Liters

Table II

QUANTITIES AND UNITS OF MECHANICS

Multiply	By	To obtain
MASS		
Grains (1/7,000 lb)	64.79891 (exactly)	Milligrams
Troy ounces (480 grains)	31.1035	Grams
Ounces (avdp)	28.3495	Grams
Pounds (avdp)	0.45359237 (exactly)	Kilograms
Short tons (2,000 lb)	907.185	Kilograms
	0.907185	Metric tons
Long tons (2,240 lb)	1,016.05	Kilograms
FORCE/AREA		
Pounds per square inch	0.070307	Kilograms per square centimeter
	0.689476	Newtons per square centimeter
Pounds per square foot	4.88243	Kilograms per square meter
	47.8803	Newtons per square meter
MASS/VOLUME (DENSITY)		
Ounces per cubic inch	1.72999	Grams per cubic centimeter
Pounds per cubic foot	16.0185	Kilograms per cubic meter
	0.0160185	Grams per cubic centimeter
Tons (long) per cubic yard	1.32894	Grams per cubic centimeter
MASS/CAPACITY		
Ounces per gallon (U.S.)	7.4893	Grams per liter
Ounces per gallon (U.K.)	6.2362	Grams per liter
Pounds per gallon (U.S.)	119.829	Grams per liter
Pounds per gallon (U.K.)	99.779	Grams per liter
BENDING MOMENT OR TORQUE		
Inch-pounds	0.011521	Meter-kilograms
	1.12985×10^{6}	Centimeter-dynes
Foot-pounds	0.138255	Meter-kilograms
	1.35582×10^{7}	Centimeter-dynes
Foot-pounds per inch	5.4431	Centimeter-kilograms per centimeter
Ounce-inches	72.008	Gram-centimeters
VELOCITY		
Feet per second	30.48 (exactly)	Centimeters per second
	0.3048 (exactly)*	Meters per second
Feet per year	0.965873×10^{-6}*	Centimeters per second
Miles per hour	1.609344 (exactly)	Kilometers per hour
	0.44704 (exactly)	Meters per second
ACCELERATION*		
Feet per second^2	0.3048*	Meters per second^2
FLOW		
Cubic feet per second (second-feet)	0.028317*	Cubic meters per second
Cubic feet per minute	0.4719	Liters per second
Gallons (U.S.) per minute	0.06309	Liters per second
FORCE*		
Pounds	0.453592*	Kilograms
	4.4482*	Newtons
	4.4482×10^{-5}*	Dynes

Multiply	By	To obtain
WORK AND ENERGY*		
British thermal units (Btu)	0.252*	Kilogram calories
	1,055.06	Joules
Btu per pound	2.326 (exactly)	Joules per gram
Foot-pounds	1.35582*	Joules
POWER		
Horsepower	745.700	Watts
Btu per hour	0.293071	Watts
Foot-pounds per second	1.35582	Watts
HEAT TRANSFER		
Btu in./hr ft^2 deg F (k, thermal conductivity)	1.442	Milliwatts/cm deg C
	0.1240	Kg cal/hr m deg C
Btu ft/hr ft^2 deg F	1.4880*	Kg cal m/hr m^2 deg C
Btu/hr ft^2 deg F (C, thermal conductance)	0.568	Milliwatts/cm^2 deg C
	4.882	Kg cal/hr m^2 deg C
Deg F hr ft^2/Btu (R, thermal resistance)	1.761	Deg C cm^2/milliwatt
Btu/lb deg F (c, heat capacity)	4.1868	J/g deg C
Btu/lb deg F	1.000*	Cal/gram deg C
Ft^2/hr (thermal diffusivity)	0.2581	Cm^2/sec
	0.09290*	M^2/hr
WATER VAPOR TRANSMISSION		
Grains/hr ft^2 (water vapor transmission)	16.7	Grams/24 hr m^2
Perms (permeance)	0.659	Metric perms
Perm-inches (permeability)	1.67	Metric perm-centimeters

Table III

OTHER QUANTITIES AND UNITS

Multiply	By	To obtain
Cubic feet per square foot per day (seepage)	304.8*	Liters per square meter per day
Pound-seconds per square foot (viscosity)	4.8824*	Kilogram second per square meter
Square feet per second (viscosity)	0.092903*	Square meters per second
Fahrenheit degrees (change)*	5/9 exactly	Celsius or Kelvin degrees (change)*
Volts per mil	0.03937	Kilovolts per millimeter
Lumens per square foot (foot-candles)	10.764	Lumens per square meter
Ohm-circular mils per foot	0.001662	Ohm-square millimeters per meter
Millicuries per cubic foot	35.3147*	Millicuries per cubic meter
Milliamps per square foot	10.7639*	Milliamps per square meter
Gallons per square yard	4.527219*	Liters per square meter
Pounds per inch	0.17858*	Kilograms per centimeter

GPO 855-412

ABSTRACT

Draft-tube surge experiments were conducted with models of draft tubes, using air as the fluid. The occurrence, frequency, and amplitude of surges were correlated with flow and draft-tube geometry variables. Studies show that surges arise when angular momentum reaches a critical value relative to linear momentum. Surge frequency and peak-to-peak pressures are independent of viscous effects for Reynolds numbers above 80,000, and are correlated with a dimensionless momentum parameter for a particular draft-tube shape. A criterion is given for predicting the surging threshold. Results of the study are applied to analysis of draft-tube surging in the Fontenelle and Hoover replacement turbines.

ABSTRACT

Draft-tube surge experiments were conducted with models of draft tubes, using air as the fluid. The occurrence, frequency, and amplitude of surges were correlated with flow and draft-tube geometry variables. Studies show that surges arise when angular momentum reaches a critical value relative to linear momentum. Surge frequency and peak-to-peak pressures are independent of viscous effects for Reynolds numbers above 80,000, and are correlated with a dimensionless momentum parameter for a particular draft-tube shape. A criterion is given for predicting the surging threshold. Results of the study are applied to analysis of draft-tube surging in the Fontenelle and Hoover replacement turbines.

ABSTRACT

Draft-tube surge experiments were conducted with models of draft tubes, using air as the fluid. The occurrence, frequency, and amplitude of surges were correlated with flow and draft-tube geometry variables. Studies show that surges arise when angular momentum reaches a critical value relative to linear momentum. Surge frequency and peak-to-peak pressures are independent of viscous effects for Reynolds numbers above 80,000, and are correlated with a dimensionless momentum parameter for a particular draft-tube shape. A criterion is given for predicting the surging threshold. Results of the study are applied to analysis of draft-tube surging in the Fontenelle and Hoover replacement turbines.

ABSTRACT

Draft-tube surge experiments were conducted with models of draft tubes, using air as the fluid. The occurrence, frequency, and amplitude of surges were correlated with flow and draft-tube geometry variables. Studies show that surges arise when angular momentum reaches a critical value relative to linear momentum. Surge frequency and peak-to-peak pressures are independent of viscous effects for Reynolds numbers above 80,000, and are correlated with a dimensionless momentum parameter for a particular draft-tube shape. A criterion is given for predicting the surging threshold. Results of the study are applied to analysis of draft-tube surging in the Fontenelle and Hoover replacement turbines.

Hyd-591
Cassidy, J. J.
EXPERIMENTAL STUDY AND ANALYSIS OF DRAFT-TUBE SURGING
Bur Reclam Lab Rep Hyd-591, Hydraul Br, May 1969. Bureau of Reclamation, Denver, 9 p, 20 fig, 3 tab, 13 ref

DESCRIPTORS—/ *draft tubes/ *turbines/ *hydroelectric plants/ hydraulic machinery/ fluid mechanics/ dimensional analysis/ *surges/ air/ unsteady flow/ pressure/ laboratory tests/ model tests/ fluid flow/ non-uniform flow
IDENTIFIERS—/ fluid dynamics/ hydraulic resonance

Hyd-591
Cassidy, J. J.
EXPERIMENTAL STUDY AND ANALYSIS OF DRAFT-TUBE SURGING
Bur Reclam Lab Rep Hyd-591, Hydraul Br, May 1969. Bureau of Reclamation, Denver, 9 p, 20 fig, 3 tab, 13 ref

DESCRIPTORS—/ *draft tubes/ *turbines/ *hydroelectric plants/ hydraulic machinery/ fluid mechanics/ dimensional analysis/ *surges/ air/ unsteady flow/ pressure/ laboratory tests/ model tests/ fluid flow/ non-uniform flow
IDENTIFIERS—/ fluid dynamics/ hydraulic resonance

Hyd-591
Cassidy, J. J.
EXPERIMENTAL STUDY AND ANALYSIS OF DRAFT-TUBE SURGING
Bur Reclam Lab Rep Hyd-591, Hydraul Br, May 1969. Bureau of Reclamation, Denver, 9 p, 20 fig, 3 tab, 13 ref

DESCRIPTORS—/ *draft tubes/ *turbines/ *hydroelectric plants/ hydraulic machinery/ fluid mechanics/ dimensional analysis/ *surges/ air/ unsteady flow/ pressure/ laboratory tests/ model tests/ fluid flow/ non-uniform flow
IDENTIFIERS—/ fluid dynamics/ hydraulic resonance

Hyd-591
Cassidy, J. J.
EXPERIMENTAL STUDY AND ANALYSIS OF DRAFT-TUBE SURGING
Bur Reclam Lab Rep Hyd-591, Hydraul Br, May 1969. Bureau of Reclamation, Denver, 9 p, 20 fig, 3 tab, 13 ref

DESCRIPTORS—/ *draft tubes/ *turbines/ *hydroelectric plants/ hydraulic machinery/ fluid mechanics/ dimensional analysis/ *surges/ air/ unsteady flow/ pressure/ laboratory tests/ model tests/ fluid flow/ non-uniform flow
IDENTIFIERS—/ fluid dynamics/ hydraulic resonance

REPORT NO. HYD-591
HYDRAULICS BRANCH
DIVISION OF RESEARCH